Kinetic impedance and depairing in thin and narrow superconducting films

John R. Clem and V. G. Kogan

Ames Laboratory–DOE and Department of Physics and Astronomy, Iowa State University, Ames, Iowa 50011, USA

(Received 26 July 2012; revised manuscript received 15 November 2012; published 30 November 2012)

We use both Eilenberger-Usadel and Ginzburg-Landau (GL) theory to calculate the superfluid's temperature-dependent kinetic inductance for all currents up to the depairing current in thin and narrow superconducting films. The calculations apply to BCS weak-coupling superconductors with isotropic gaps and transport mean-free paths much less than the BCS coherence length. The kinetic inductance is calculated for the response to a small alternating current when the film is carrying a dc bias current. In the slow-experiment/fast-relaxation limit, in which the superconducting order parameter quasistatically follows the time-dependent current, the kinetic inductance diverges as the bias current approaches the depairing value. However, in the fast-experiment/slow-relaxiation limit, in which the the superconducting order parameter remains fixed at a value corresponding to the dc bias current, the kinetic inductance rises to a finite value at the depairing current. We then use time-dependent GL theory to calculate the kinetic impedance of the superfluid, which includes not only the kinetic reactance, but also the kinetic resistance of the superfluid arising from dissipation due to order-parameter relaxation. The kinetic resistance is largest for angular frequencies ω obeying $\omega\tau_s > 1$, where τ_s is the order-parameter relaxation time, and for bias currents close to the depairing current. We also include the normal fluid's contribution to dissipation in deriving an expression for the total kinetic impedance. The Appendices contain many details about the temperature-dependent behavior of superconductors carrying current up to the depairing value.

DOI: 10.1103/PhysRevB.86.174521 PACS number(s): 74.78.Na, 74.25.F−, 74.25.Sv

I. INTRODUCTION

The kinetic inductance, arising chiefly from the kinetic energy of the superfluid, plays an important role in superconducting devices fabricated using thin and narrow superconducting films.[1–3] In such cases, the kinetic inductance is generally much larger than the geometric inductance arising from stored magnetic energy.[4–6] For example, the kinetic inductance plays a prominent role in determining the reset time of superconducting single-photon detectors (SSPDs) fabricated with meandering superconducting lines.[7–9] Various calculations of the kinetic inductance, relevant to the performance of microstrip resonators[10] and microwave kinetic inductance detectors (MKIDs),[11] have been carried out using (a) the London equations neglecting the current-induced suppression of the order parameter,[4–6,12] (b) the Ginzburg-Landau (GL) equations,[2,13,14] (c) a GL-inspired London-equation approach accounting for the current-induced suppression of the order parameter,[15,16] and (d) the BCS theory.[2,10] Our goal in this paper is to present theoretical calculations of the kinetic inductance for all temperatures and for all currents up to the depairing current for sample dimensions and properties applicable to present experimental studies of SSPDs (Refs. 7 and 17) and microresonators.[2] Because these studies have used thin high-resistance films of NbN,[1,2,7–9,18] Nb,[2] NbTiN,[19] and TaN (Refs. 20 and 21) in the dirty limit, we adopt an isotropic s-wave BCS description, although many of our results can be extended to apply under more general assumptions.

We consider thin ($d \ll \lambda_0$) superconducting films of width W much less than the two-dimensional screening length (Pearl length[22]) $\Lambda = 2\lambda_0^2/d$, where λ_0 is the temperature-dependent weak-field London penetration depth and d is the film thickness. The condition $W \ll \Lambda$ guarantees that the self-field generated by the current has a negligible effect upon the current density $\boldsymbol{j}$, which therefore flows with the same spatial distribution as in the normal state.[23] Moreover, this condition also guarantees that the inductance $L = L_m + L_k$ is dominated by the kinetic inductance of the superfluid L_k, which is typically larger than the geometric inductance L_m (associated with the energy stored in the magnetic field) by a factor of order Λ/W.[4] We focus on the calculation of the superfluid's kinetic inductivity $\mathcal{L}_k$. For a long strip of length ℓ, width W, and thickness d, the kinetic inductance is $L_k = \mathcal{L}_k \ell/Wd$.

When the superconductor carries such a low current that the superconducting order parameter is not significantly suppressed, the electromagnetic behavior is well described by the London equation, and the kinetic energy density of the superfluid in the clean case can be expressed as[5]

$$U_k = \frac{1}{2} n_{s0} m v_s^2 = \frac{1}{2}\left(\frac{m}{n_{s0}e^2}\right) j_s^2 = \frac{1}{2}\mu_0\lambda_0^2 j_s^2 = \frac{1}{2}\mathcal{L}_{k0} j_s^2, \tag{1}$$

where n_{s0} is the superfluid density, m the electron mass, v_s the superfluid velocity component in the x direction, $j_s = -n_{s0} e v_s$ the supercurrent density component in the x direction, and $-e$ the electron charge, such that the kinetic inductivity of the superfluid obeys[24,25]

$$\mathcal{L}_{k0}(T) = \mu_0\lambda_0^2(T) = m/n_{s0}e^2. \tag{2}$$

The subscripts 0 on n_{s0}, λ_0, and $\mathcal{L}_{k0}$ are a reminder that these quantities apply in the limit as $j_s \to 0$. The simple relationship given in Eq. (2) has made possible the determination of $\lambda_0(T)$ versus T in $YBa_2Cu_3O_{7-\delta}$ from kinetic-inductance measurements.[26]

When the superconductor carries high currents, however, calculation of the superfluid's kinetic inductance becomes more complicated, especially when the current density approaches the depairing value j_d. In high currents, it is no longer possible to define the kinetic inductance by considering only the stored kinetic energy density as in Eq. (1) because, as

examined in detail in Appendix D, increasing j_s to large values also affects the superconducting condensation energy by suppressing the superconducting order parameter. To account for this effect, we take advantage of Maki's[27–29] recognition that the current-induced suppression of the order parameter in a thin film can be treated using a pair-breaking parameter exactly analogous to that used by Abrikosov and Gor'kov[30] in their study of the effect of paramagnetic impurities upon superconductivity. The fusion of the theories for these two problems[31] has resulted in a large body of related work,[32–37] much of which we summarize for the benefit of the reader in Sec. II and the Appendices. As noted by previous authors,[38–42] a convenient starting point for this purpose is the Eilenberger-Usadel theory.[43,44]

An additional complication in calculating the kinetic inductance is that n_s, which depends on the superconducting order parameter, can change only on a time scale slower than a variety of difficult-to-determine internal relaxation times,[13,24,45,46] which we here represent crudely by a single relaxation time τ_s. As a consequence, n_s may or may not be able to follow the changes in j_s and v_s.

Calculations of the current dependence of $\mathcal{L}_k$ are simplified in two limiting cases[13]: (a) slow experiments (fast relaxation, Sec. III), in which j_s and v_s vary on an experimental time scale $\tau_{\rm expt}$ much longer than the relaxation time τ_s, such that the order parameter and the superfluid density n_s quasistatically follow j_s and v_s, and (b) fast experiments (slow relaxation, Sec. IV), in which j_s and v_s change so rapidly about their time averages $\bar{j}_s$ and $\bar{v}_s$ (on a time scale $\tau_{\rm expt}$ much shorter than τ_s) that the order parameter and n_s cannot track the time dependence, and n_s remains very close to the value corresponding to $\bar{j}_s$ and $\bar{v}_s$. To provide an approximation to the transition between these two limiting cases, in Sec. V we employ a simplified phenomenological model based on the time-dependent GL (TDGL) equations[24] to calculate the complex impedivity due to the superfluid. In Sec. VI, we include the normal-fluid's resistive contribution to the total complex impedivity, and in Sec. VII we provide a brief summary and discussion of our results. Various details of the calculation are included in Appendices A–D.

II. SUPERFLUID-VELOCITY DEPENDENCE OF THE SUPERCURRENT DENSITY AND THE DEPAIRING-CURRENT DENSITY

The purpose of this section is to explain clearly how to calculate the many effects of the current-induced suppression of the order parameter that have been obtained by previous authors. We need a formalism that allows us to calculate the depairing-current density $j_d(T)$ in superconductors with a short normal-state mean-free path at all temperatures in the superconducting state. A compact way of doing this is to employ the quasiclassical Eilenberger[43] theory as formulated by Usadel[44] for the dirty limit.

Consider a superconducting strip extending along the x direction when the current is uniform. Let j_s and $A_s = mv_s/e$ denote the x components of the supercurrent density $\boldsymbol{j}_s$ and the gauge-invariant vector potential $\boldsymbol{A}_s = \boldsymbol{A} + (\phi_0/2\pi)\boldsymbol{\nabla}\gamma$, where $\boldsymbol{A}$ is the gauge-dependent vector potential, $\phi_0 = h/2e$ the superconducting flux quantum, and γ the gauge-dependent phase of the superconducting order parameter.

The supercurrent density can always be expressed as $j_s = -n_s e v_s$, but in general n_s is a function of the superfluid velocity v_s and has the value n_{s0} when $v_s = 0$ but decreases monotonically to zero as $|v_s|$ increases. For positive j_s and negative values of v_s, the supercurrent density $j_s = n_s e|v_s|$ initially increases linearly as a function of $|v_s|$, reaches a maximum $j_d(T)$ (the depairing or pair-breaking current density) at $|v_s| = v_d(T)$, then decreases to zero at $|v_s| = v_m(T)$.

When the superconductor is current biased, only the portion of the curve j_s versus $|v_s|$ for $0 \leqslant |v_s| \leqslant v_d(T)$ is accessible. On the other hand, following a suggestion by Fulde and Ferrell,[47] Bhatnagar and Stern[48,49] showed that it is possible to probe experimentally the shape of j_s versus $|v_s|$ even for $v_d(T) \leqslant |v_s| \leqslant v_m(T)$ using a multiply connected sample geometry. In this paper, we first examine the behavior of j_s over the full range of values of v_s, but later in applying these results to study the kinetic inductance we limit our attention to the current-biased case in which j_s is a single-valued function of v_s in the range $0 \leqslant j_s \leqslant j_d$.

A. Depairing-current density calculated from the Usadel equations

For the problem at hand, the Usadel equations can be written as[44]

$$-\hbar D(GF' - FG')' = 2\Delta G - 2\hbar\omega_n F\,, \tag{3}$$

$$G^2 + |F|^2 = 1\,, \tag{4}$$

$$\Delta\,\ln\frac{T_{c0}}{T} = 2\pi k_B T\sum_{n=0}^{\infty}\left(\frac{\Delta}{\hbar\omega_n} - F\right)\,, \tag{5}$$

$$j_s = -4\pi e N(0) D k_B T\sum_{n=0}^{\infty}\mathrm{Im}F^*F'\,, \tag{6}$$

where Δ is the superconducting order parameter, $D = v_F^2\tau/3 = v_F\ell/3$ is the diffusivity, v_F is the average velocity of electrons at the Fermi surface, τ is the normal-state transport lifetime, ℓ is the mean-free path, $\hbar\omega_n = (2n+1)\pi k_B T$ is the Matsubara frequency, $N(0)$ is the density of Bloch states of one spin at the Fermi level, T is the temperature, and T_{c0} is the zero-current transition temperature. The primes in Eq. (3) denote differentiation with respect to x. These equations describe supercurrent flow in a superconductor with an s-wave isotropic gap in the weak-coupling limit of the BCS theory.[50] However, this mean-field theory does not account for the possibility that one- or two-dimensional fluctuations could grow to produce phase slips or vortex crossings.

Since $W \ll \Lambda$, we can neglect the self-field of the current and choose a gauge for which we may replace the gauge-invariant gradient $\boldsymbol{\nabla} + 2\pi i\boldsymbol{A}/\phi_0$ by $\hat{x}\partial_x$. Looking for solutions of the form $\Delta = \Delta_q e^{iqx}$, $F = F_{nq}e^{iqx}$, and $G = G_{nq}$, where q is the gradient of the phase of the order parameter, we find that Eqs. (3) and (4) become

$$QF_{nq}G_{nq} = \Delta_q G_{nq} - \hbar\omega_n F_{nq}, \tag{7}$$

$$G_{nq}^2 + F_{nq}^2 = 1, \tag{8}$$

where $Q = \hbar D q^2/2$.

Throughout this paper, the symbol q appears frequently; it can be regarded as a compact abbreviation for the gauge-invariant vector potential A_s, the superfluid velocity v_x, or the gradient of the phase γ of the order parameter, since all these quantities are related via $q = 2\pi A_s/\phi_0 = 2mv_s/\hbar = \gamma/x$. The presence of a subscript q indicates that the subscripted quantity is a function of q. We show later that as q increases, the pair-breaking effect reduces the superconducting transition temperature T_{cq}, the order parameter Δ_q (Figs. 1 and 5) and the superfluid density n_{sq} (Fig. 2), and increases the penetration depth λ_q [Eq. (17)]. We show here that these q dependencies combine to produce the current dependence of the kinetic inductance shown in Figs. 7 and 8. However, the q dependence of λ_q could be shown somewhat more directly in sensitive measurements of the penetration depth in the Meissner state as a function of applied ac and dc magnetic fields.

As noted by Maki,[37] Eqs. (7) and (8) are equivalent to those of the Abrikosov-Gor'kov (AG) theory[30] for pair-breaking scattering, except for the replacement of the AG spin-flip scattering rate $1/\tau_m$ by $Dq^2/2$. Our results therefore share many properties with those of the AG theory. For example, we show that the transition temperature T_{cq} depends upon q and decreases monotonically from its value T_{c0} at $q = 0$ to zero at a critical value of q given by $q_m(0) = 1/\xi(0) = (\pi\xi_0\ell/3)^{-1/2}$, where $\xi_0 = \hbar v_F/\pi\Delta_0(0)$ is the BCS coherence length.[50] For a fixed value of q, the order parameter $\Delta_q(T)$ is nonzero only for temperatures T less than T_{cq}; equivalently, for a fixed temperature T, the order parameter $\Delta_q(T)$ is nonzero only for values of q less than $q_m(T) = 1/\xi(T)$.

Introducing $u_{nq} = G_{nq}/F_{nq}$, we find that Eqs. (7) and (8) can be written as

$$\frac{\eta}{\epsilon} = u_{nq}\left(1 - \frac{\zeta}{\sqrt{1+u_{nq}^2}}\right) \tag{9}$$

and

$$F_{nq} = \frac{1}{\sqrt{1+u_{nq}^2}}, \tag{10}$$

where $\eta = n + 1/2$, $\epsilon = \Delta_q/2\pi k_B T$, and $\zeta = Q/\Delta_q$. u_{nq} (which depends implicitly upon T) can be obtained for arbitrary values of η, ϵ, and ζ by solving Eq. (9) as a quartic equation (see Appendix A).

With the introduction of u_{nq}, two equations remain to be solved. The self-consistency equation (5) in the presence of the current becomes, for general values of Δ_q, ω, Q, and T,

$$\ln\frac{1}{t} = \sum_{n=0}^{\infty}\left(\frac{1}{n+1/2} - \frac{1}{\epsilon\sqrt{1+u_{nq}^2}}\right). \tag{11}$$

In general, $\Delta_q(T)$ must be obtained by numerically solving Eq. (11) using Eq. (A2), but the results can be checked against analytic results obtainable in the limits of $q \to 0$ and $q \to q_m(T)$. Figure 1 shows $[\Delta_q(T)/\Delta_0(0)]^2$ as a function of $q/q_m(0)$ for a series of values of the reduced temperature $t = T/T_{c0}$. (Closely related plots were given as Fig. 1 in Ref. 32 and Fig. 4 in Ref. 33.) The sums for $t \geqslant 0.1$ were evaluated by summing n from 0 to 500, but for $t = 0$ we used the analytic results in Eqs. (23)–(25).

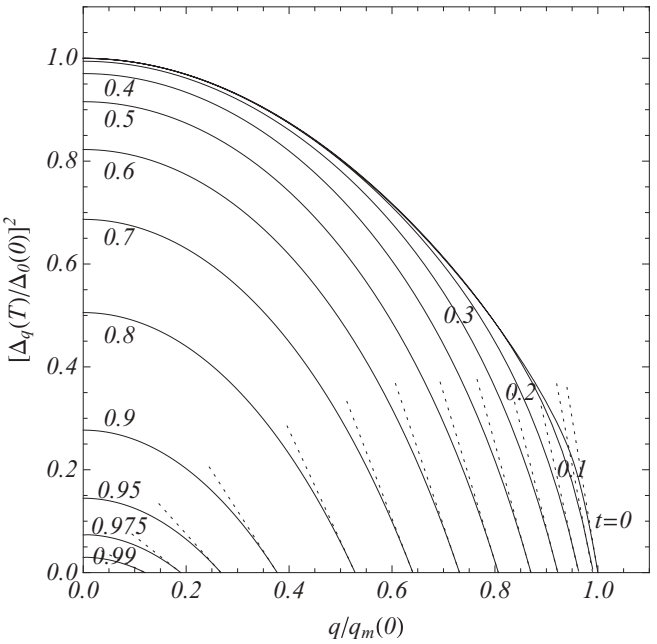

FIG. 1. $[\Delta_q(T)/\Delta_0(0)]^2$ vs $q/q_m(0)$ obtained from Eqs. (11) and (A2) for various values of $t = T/T_{c0}$. The dotted lines show the linear behavior as $[\Delta_q(T)/\Delta_0(0)]^2 \to 0$ in the limit as $q \to q_m(T)$.

From the current equation (6) we find that when the superfluid velocity v_s is in the x direction, the supercurrent density in that direction is[25]

$$j_{sq}(T) = -n_{sq}(T)ev_s. \tag{12}$$

From Eqs. (6), (10), and (12), we obtain a general expression for the q-dependent superfluid density,

$$n_{sq}(T) = \frac{8\pi mN(0)Dk_BT}{\hbar}\sum_{n=0}^{\infty}\frac{1}{1+u_{nq}^2}. \tag{13}$$

When $q \to 0$, we have $u_{n0} = 2\pi k_B T(n+1/2)/\Delta_0(T)$ [see Eq. (9)], and when this is used in Eq. (13), evaluation of the sum yields

$$n_{s0}(T) = \frac{2\pi mN(0)D\Delta_0(T)}{\hbar}\tanh\left(\frac{\Delta_0(T)}{2k_BT}\right), \tag{14}$$

such that

$$n_{s0}(0) = \frac{2\pi mN(0)D\Delta_0(0)}{\hbar} \tag{15}$$

and

$$\frac{n_{sq}(T)}{n_{s0}(0)} = \frac{4k_BT}{\Delta_0(0)}\sum_{n=0}^{\infty}\frac{1}{1+u_{nq}^2}. \tag{16}$$

In general, $n_{sq}(T)/n_{s0}(0)$ must be obtained by numerically solving Eqs. (11) and (16) using Eq. (A2). Figure 2 shows $n_{sq}(T)/n_{s0}(0)$ as a function of $q/q_m(0)$ for a series of values of the reduced temperature $t = T/T_{c0}$. The sums for $t \geqslant 0.1$ were evaluated by summing n from 0 to 500, but for $t = 0$ we used the analytic results in Eqs. (26) and (27).

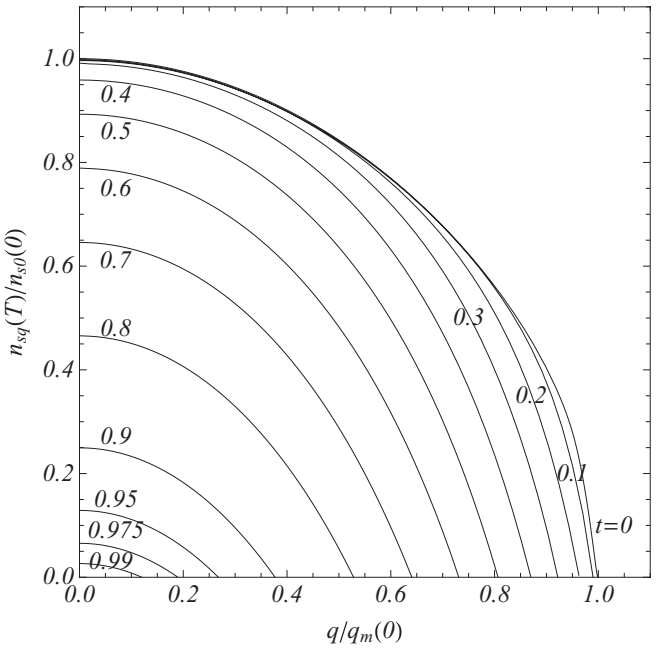

FIG. 2. $n_{sq}(T)/n_{s0}(0) = \lambda_0^2(0)/\lambda_q^2(T)$ vs $q/q_m(0)$ obtained from Eqs. (11), (16), and (A2) for various values of $t = T/T_{c0}$. $n_{sq}(T)/n_{s0}(0) \to 0$ as $q \to q_m(T)$.

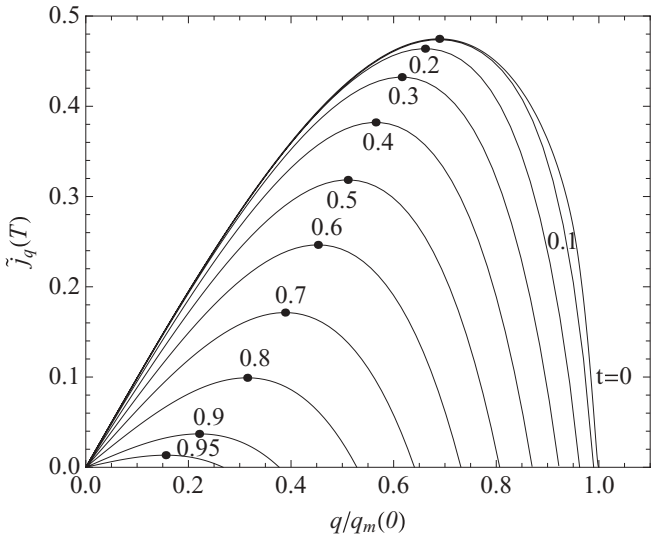

FIG. 3. $\tilde{j}_q(T)$ vs $q/q_m(0)$ obtained from Eqs. (11), (16), (19), and (A2) for various values of $t = T/T_{c0}$. The points label the values of $\tilde{j}_q$ and q corresponding to the depairing-current density j_d and q_d. Current-biased experiments probe only the portions of the curves to the left of these points. $\tilde{j}_q(T) \to 0$ as $q \to q_m(T)$.

As shown in Fig. 2, $n_{sq}(T)/n_{s0}(0)$ depends upon q and vanishes at $q = q_m(T)$ (see Appendix C). The corresponding q-dependent penetration depth $\lambda_q(T)$ can be obtained from

$$\frac{n_{sq}(T)}{n_{s0}(0)} = \frac{\lambda_0^2(0)}{\lambda_q^2(T)}. \tag{17}$$

Note, however, that current-biased experiments can access values of q only up to $q_d(T)$, where the magnitude of the current density reaches the depairing limit $j_d(T)$.

The general expression for the supercurrent density is

$$j_{sq}(T) = -\frac{n_{sq}(T)e^2A_s}{m} = -\frac{A_s}{\mu_0\lambda_q^2(T)}. \tag{18}$$

From Eq. (12) or (18) we see that, because $j_{sq}(T)$ is the product of $n_{sq}(T)$ (a monotonically decreasing function of q) and $ev_s = e^2A_s/m = e\hbar q/2m$, the magnitude of $j_{sq}(T)$ reaches a maximum, called the depairing-current density $j_d(T)$, when $q = q_d(T)$, where $0 < q_d(T) < q_m(T)$. We define $\tilde{j}_q(T)$ as the magnitude of $j_{sq}(T)$ normalized to $n_{s0}(0)ev_m(0) = \phi_0/2\pi\mu_0\lambda_0(0)^2\xi(0)$, such that

$$\tilde{j}_q(T) = \frac{n_{sq}(T)}{n_{s0}(0)}\frac{q}{q_m(0)}. \tag{19}$$

The maximum value of $\tilde{j}_q(T)$ versus q is the normalized depairing-current density $\tilde{j}_d(T)$.

In general, $\tilde{j}_q(T)$ must be obtained numerically from Eqs. (11), (16), (19), and (A2), but the results can be checked against analytic results obtainable in the limits $t \to 0$ and $t \to 1$, to be discussed in more detail later in Secs. II B and II C. Figure 3 shows the general behavior of $\tilde{j}_q(T)$ as a function of $q/q_m(0)$ for a series of values of the reduced temperature $t = T/T_{c0}$. (Plots similar to Fig. 3 were shown as Fig. 1 in Ref. 28 and Fig. 2 in Ref. 39.) The points label the values of $\tilde{j}_q$ and q corresponding to the depairing-current density j_d and q_d. The solid curve in Fig. 4 shows $[j_d(T)/j_d(0)]^{2/3} = [\tilde{j}_d(T)/\tilde{j}_d(0)]^{2/3}$ as a function of $t = T/T_{c0}$, and the dotted line illustrates how $j_c(T)$ approaches the $(1-t)^{2/3}$ behavior in the GL regime close to T_{c0}.

For all temperatures below T_{c0}, estimates of $j_d(T)$ can be obtained from

$$j_d(T) = p_d(T)\frac{\phi_0}{2\pi\mu_0\lambda_0^2(T)\xi(T)}, \tag{20}$$

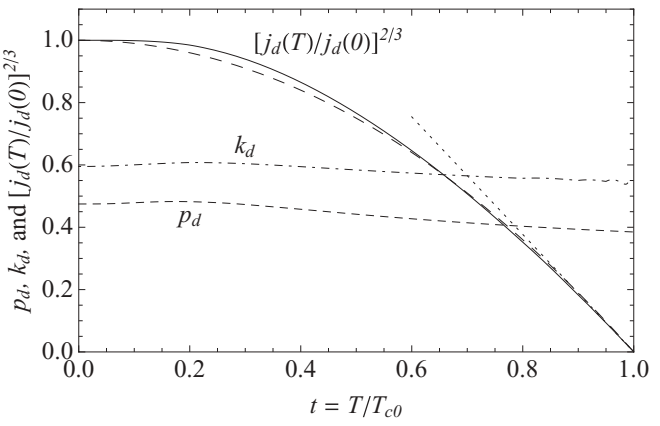

FIG. 4. $[j_d(T)/j_d(0)]^{2/3}$ (solid) vs $t = T/T_{c0}$ obtained numerically from Eqs. (11), (16), (19), and (A2). The dotted line shows the behavior of $j_d(T)$ in the GL limit near T_{c0} [Eq. (41)], and the long-dashed curve shows the approximation (Refs. 39, 51, and 52) $j_d(T)/j_d(0) \approx (1-t^2)^{3/2}$. The short-dashed curve shows the variation of $p_d(T)$ [Eq. (20)] from 0.475 at $t = 0$ to 0.385 at $t = 1$, and the dotted-dashed curve shows the variation of $k_d(T)$ [Eq. (21)] from 0.595 at $t = 0$ to 0.544 at $t = 1$.

where $p_d(T)$ is a dimensionless function defined by Eq. (20). The dashed curve in Fig. 4 shows $p_d(T)$, which is obtained numerically from all the other quantities in Eq. (20), varying from 0.475 at $T = 0$ [Eq. (30)] to 0.385 as $T \to T_{c0}$ [Eq. (42)] with a maximum of 0.483 at $t = T/T_{c0} = 0.17$.

Similarly, estimates of the depairing-current density also can be obtained for all temperatures from

$$j_d(T) = k_d(T) H_c(T)/\lambda_0(T), \tag{21}$$

where the dimensionless quantity $k_d(T)$, defined by Eq. (21) and shown by the dotted-dashed curve in Fig. 4, varies from 0.595 at $T = 0$ [Eq. (30)] to 0.544 as $T \to T_{c0}$ [Eq. (42)] with a maximum of 0.608 at $t = T/T_{c0} = 0.21$. The values of k_d shown in Fig. 4 were obtained from

$$k_d(T) = 0.595 \frac{\tilde{j}_d(T)}{\tilde{j}_d(0)} \frac{H_c(0)}{H_c(T)} \frac{\lambda_0(T)}{\lambda_0(0)} \tag{22}$$

via Eqs. (32), (D16), and (B2), where $H_c(T)$ is the temperature-dependent bulk thermodynamic critical field (see Appendix D). Plots similar to Fig. 4 were given as Fig. 9 in Ref. 38 and Fig. 4 in Ref. 39.

B. Depairing-current density at zero temperature

At $T = 0$, the q dependence of $\Delta_q(0)$ can be obtained by converting the sum in Eq. (11) to an integral over u_{nq}. The result is[30,37]

$$\frac{\Delta_q(0)}{\Delta_0(0)} = \exp(-\pi\zeta_0/4), \quad 0 \leqslant \zeta_0 \leqslant 1 \tag{23}$$

$$= \exp\left[-\left(\zeta_0 \sin^{-1}\zeta_0^{-1} - \sqrt{1-\zeta_0^{-2}}\right)/2 - \cosh^{-1}\zeta_0\right], \quad \zeta_0 \geqslant 1 \tag{24}$$

where

$$\zeta_0 = \frac{\hbar D q^2}{2\Delta_q(0)} = \frac{1}{2}\left(\frac{q}{q_m(0)}\right)^2 \frac{\Delta_0(0)}{\Delta_q(0)}. \tag{25}$$

Figure 5 shows $[\Delta_q(0)/\Delta_0(0)]^2$, obtained from numerical solution of Eqs. (23)–(25), as a function of $q/q_m(0) = v_s/v_m(0)$.

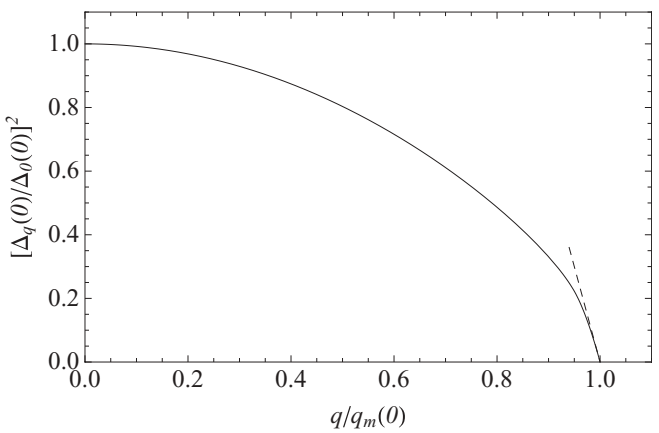

FIG. 5. $[\Delta_q(0)/\Delta_0(0)]^2$ vs $q/q_m(0)$ obtained from Eqs. (23)–(25). The dashed line shows the linear behavior $6[1 - q/q_m(0)]$ as $q \to q_m(0)$.

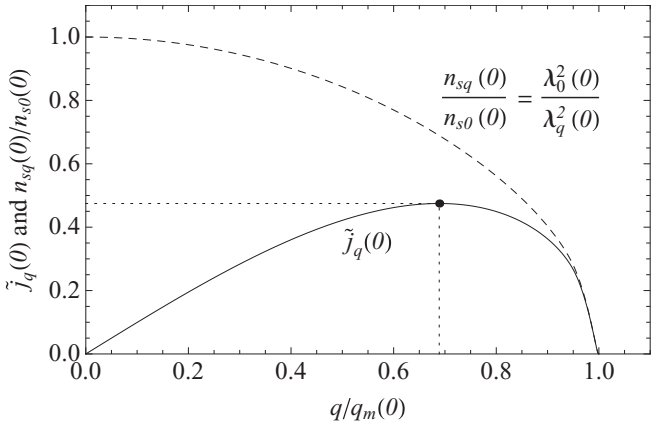

FIG. 6. Reduced superfluid density $n_{sq}(0)/n_{s0}(0) = \lambda_0^2(0)/\lambda_q^2(0)$ (dashed curve) vs $q/q_m(0) = v_s/v_m(0)$, obtained from Eqs. (26) and (27), and normalized q-dependent supercurrent density $\tilde{j}_q(0)$ (solid curve) vs $q/q_m(0) = v_s/v_m(0)$, obtained from Eq. (29). The black point and dotted lines indicate the maximum $\tilde{j}_q(0)$, the normalized depairing-supercurrent density $\tilde{j}_d = 0.475$, which occurs at $q_d/q_m(0) = 0.689$.

The q dependence of $n_{sq}(0)$ can be obtained in a similar way. The result is[37]

$$\frac{n_{sq}(0)}{n_{s0}(0)} = \exp(-\pi\zeta_0/4)(1 - 4\zeta_0/3\pi), \quad 0 \leqslant \zeta_0 \leqslant 1 \tag{26}$$

$$= \exp(-\pi\zeta_0/4)\left\{\frac{2}{3\pi\zeta_0^2}\left[\left(1+2\zeta_0^2\right)\sqrt{\zeta_0^2-1} - 2\zeta_0^3\right] + \frac{2}{\pi}\sin^{-1}\zeta_0^{-1}\right\}, \quad \zeta_0 \geqslant 1 \tag{27}$$

where ζ_0 is given by Eq. (25). $n_{sq}(0)$ is shown as the dashed curve in Fig. 6. The q-dependent penetration depth at zero temperature $\lambda_q(0)$ can be obtained from

$$\frac{n_{sq}(0)}{n_{s0}(0)} = \frac{\lambda_0^2(0)}{\lambda_q^2(0)}. \tag{28}$$

To obtain the depairing-current density, consider the q-dependent (or v_s-dependent) supercurrent density at $T = 0$ [Eq. (12)], normalized to $-n_{s0}(0)ev_m(0) = -\phi_0/2\pi\mu_0\lambda_0(0)^2\xi(0)$,

$$\tilde{j}_q(0) = \frac{n_{sq}(0)}{n_{s0}(0)}\left(\frac{q}{q_m(0)}\right), \tag{29}$$

shown as the solid curve in Fig. 6. (Plots similar to Fig. 6 were shown as Fig. 1 in Ref. 28 and Fig. 2 in Ref. 39) The point and dotted lines show the maximum $\tilde{j}_q(0)$, the normalized depairing-supercurrent density $\tilde{j}_d(0) = 0.475$, which occurs at $q_d(0)/q_m(0) = 0.689$ and $\zeta_0 = 0.300$.[28] The resulting zero-temperature depairing-supercurrent density can be expressed in several ways:

$$j_d(0) = 0.475 \frac{\phi_0}{2\pi\mu_0\lambda_0^2(0)\xi(0)} \tag{30}$$

$$= 1.491 N(0) e [\Delta_0(0)]^{3/2}\sqrt{D/\hbar} \tag{31}$$

$$= 0.595 H_c(0)/\lambda_0(0). \tag{32}$$

Equation (31) coincides with the result given for the depairing-supercurrent density in Ref. 38. Here, $H_c(T)$ is the

temperature-dependent bulk thermodynamic critical field (see Appendix D), and $H_c(0) = \Delta_0(0)\sqrt{N(0)/\mu_0}$.

C. Depairing-current density in the GL regime

As shown by Gor'kov,[53] the GL theory of superconductivity[54] is derivable from the microscopic BCS theory[50] at temperatures T close to the transition temperature T_{c0}. This assures us that we also can apply the Usadel equations to recover the GL results. We present the GL depairing-current results here for completeness, even though they are so well known that they appear in textbooks.[24] For T close to T_{cq} or, equivalently, for q close to $q_m(T)$, the q-dependent order parameter $\Delta_q(T)$ becomes small, and it is useful to expand u_{nq} and $1/\epsilon\sqrt{1+u_{nq}^2}$ in powers of $\epsilon = \Delta_q(T)/2\pi k_B T$:

$$\frac{1}{\epsilon\sqrt{1+u_{nq}^2}} = \frac{1}{\eta+\alpha} - \frac{\epsilon^2}{2}\left[\frac{1}{(\eta+\alpha)^3} - \frac{\alpha}{(\eta+\alpha)^4}\right] + O(\epsilon^4), \tag{33}$$

where

$$\alpha = \frac{e^{-\gamma}}{4t}\frac{q_m^2(T)}{q_m^2(0)} = \frac{0.140}{t}\frac{q_m^2(T)}{q_m^2(0)}. \tag{34}$$

Substituting this into Eq. (11) and keeping only the lowest-order terms, since we know that $\epsilon = \Delta_q(T)/2\pi k_B T \ll 1$ when $1-t \ll 1$, we obtain

$$\ln\frac{T_{c0}}{T} = \sum_{n=0}^{\infty}\left\{\frac{1}{n+1/2} - \frac{1}{n+1/2+\alpha} + \left[\frac{1}{(n+1/2+\alpha)^3} - \frac{\alpha}{(n+1/2+\alpha)^4}\right]\frac{\epsilon^2}{2}\right\}. \tag{35}$$

The sums can be expressed in terms of digamma functions and their derivatives. When $1-t \ll 1$, Eq. (35) has solutions only for $\alpha \ll 1$ and can be expanded as

$$1-t = \frac{\pi^2 e^{-\gamma} q^2}{8q_m^2(0)} + \frac{7\zeta(3)\epsilon^2}{2}. \tag{36}$$

Solving for ϵ^2, dividing by $\epsilon_0^2 = 2(1-t)/7\zeta(3)$, and making use of $q_m^2(T) = [8e^{\gamma}(1-t)/\pi^2]q_m^2(0)$ (see Appendix C), we obtain

$$\frac{\Delta_q^2(T)}{\Delta_0^2(T)} = 1 - \frac{q^2}{q_m^2(T)}, \tag{37}$$

where $q_m(T) = 1/\xi(T)$.

Substituting the expansion of Eq. (33) into Eq. (16), keeping only the lowest-order terms, we obtain

$$\frac{n_{sq}(T)}{n_{s0}(T)} = \frac{\lambda_0^2(T)}{\lambda_q^2(T)} = \frac{\Delta_q^2(T)}{\Delta_0^2(T)} = f^2 = 1 - \frac{q^2}{q_m^2(T)} \tag{38}$$

and

$$\frac{n_{sq}(T)}{n_{s0}(0)} = \frac{\lambda_0^2(0)}{\lambda_q^2(T)} = \frac{4\pi e^{\gamma}}{7\zeta(3)}\left(1 - \frac{q^2}{q_m^2(T)}\right)(1-t). \tag{39}$$

The reduced q-dependent supercurrent density becomes

$$\tilde{j}_q(T) = \frac{4\pi e^{\gamma}}{7\zeta(3)}\frac{q_m(T)}{q_m(0)}\left(1 - \frac{q^2}{q_m^2(T)}\right)\frac{q}{q_m(T)}(1-t), \tag{40}$$

the maximum of which occurs at $q_d(T)/q_m(T) = 1/\sqrt{3}$, such that (see Appendix C) the reduced depairing-current density is

$$\tilde{j}_d(T) = \frac{16\sqrt{2}e^{3\gamma/2}}{21\sqrt{3}\zeta(3)}(1-t)^{3/2} = 1.230(1-t)^{3/2}. \tag{41}$$

Thus, in the GL regime, the depairing-current density can be expressed as

$$j_d(T) = 0.385\frac{\phi_0}{2\pi\mu_0\lambda_0^2(T)\xi(T)}, \tag{42}$$

where $0.385 = 2/3\sqrt{3}$,

$$j_d(T) = 3.865N(0)e[\Delta_0(0)]^{3/2}\sqrt{D/\hbar}(1-t)^{3/2}, \tag{43}$$

or, since $\sqrt{2}H_c = \phi_0/2\pi\mu_0\lambda_0\xi$ in the GL theory,

$$j_d(T) = 0.544H_c(T)/\lambda_0(T), \tag{44}$$

where $0.544 = (2/3)^{3/2}$.

To simplify calculations in the GL limit, later in Secs. III and IV we introduce the parameter ϕ $(0 \leqslant \phi \leqslant \pi/2)$, such that

$$|j_{sq}|/j_d = \sin\phi, \tag{45}$$

$$q/q_m(T) = (2/\sqrt{3})\sin(\phi/3), \tag{46}$$

$$f^2 = [1 + 2\cos(2\phi/3)]/3. \tag{47}$$

III. SUPERFLUID KINETIC INDUCTIVITY IN SLOW EXPERIMENTS (FAST RELAXATION)

In Sec. II, we have summarized the results of previous authors and provided details of how to account quantitatively for the current-induced suppression of the order parameter in dirty thin-film superconductors at all temperatures in the superconducting state. We are now in a position to calculate the kinetic inductivity of the superfluid measured in slow, low-frequency (or, equivalently, fast relaxation) current-biased experiments, in which both j_s $[|j_s| \leqslant j_d(T)]$ and v_s $[|v_s| \leqslant v_d(T)]$ vary on a time scale $\tau_{\rm expt}$ much longer than the relaxation time τ_s required for the superconducting order parameter to change.[13,24,45]

In a one-dimensional conductor carrying a uniform current, the gauge-invariant electric potential $P = \Phi - (\phi_0/2\pi)d\gamma/dt$ is zero,[55] and the electric field along the conductor is $E = -dA_s/dt = \mathcal{L}_k(q,T)dj_{sq}(T)/dt$.[56] Since from Eq. (18) we have $A_s = (\phi_0/2\pi)q = -j_{sq}(T)\mu_0\lambda_q^2(T)$, taking the time derivative and using $df/dt = (df/dq)dq/dt$, we obtain the kinetic inductivity of the superfluid for slow experiments,

$$\mathcal{L}_k(q,T) = \mu_0\left[\frac{d}{dq}\left(\frac{q}{\lambda_q^2(T)}\right)\right]^{-1} = \left|\frac{dj_{sq}(T)}{dA_s}\right|^{-1} = \mu_0\lambda_0^2(T)F_s\left(\frac{|j_s|}{j_d(T)}\right), \tag{48}$$

where the slow-experiment function F_s is simply $\mathcal{L}_k(q,T)/\mu_0\lambda_0^2(T)$ but expressed as a function of the normalized current density $|j_s|/j_d(T)$ rather than as a function of q. While q is a convenient theoretical variable, j_s is a more convenient variable for the current-biased case. For

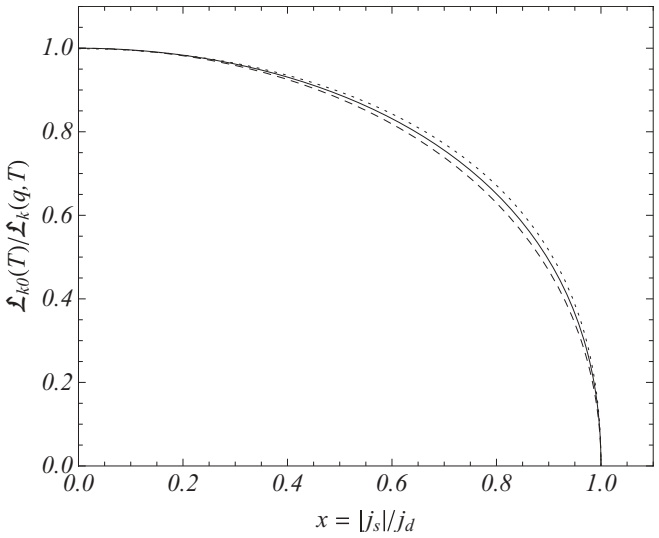

FIG. 7. $\mathcal{L}_{k0}(T)/\mathcal{L}_k(q,T) = 1/F_s[|j_s|/j_d(T)]$ for slow experiments vs $x = |j_s|/j_d(T)$ at $t = T/T_{c0} = 0$ (solid line), $t = 0.3$ (dotted line), and $t \to 1$ (dashed line). Note that $\mathcal{L}_{k0}(T) = \mathcal{L}_k(0,T) = \mu_0\lambda_0^2(T)$.

$|q| < q_d(T)$ and $|j_s| < j_d(T)$, j_s is a single-valued function of q, shown in Figs. 3 and 6.

In the limit of small currents, when $q \to 0$, $\mathcal{L}_k(q,T)$ reduces to $\mathcal{L}_k(0,T) = \mathcal{L}_{k0}(T)$ [Eq. (2)]. However, as can be seen from Figs. 3 and 6, $|dj_{sq}/dq|$ decreases monotonically for increasing values of q and becomes zero at the depairing value. Accordingly, as q increases, $\mathcal{L}_k(q,T)$ starts from $\mathcal{L}_{k0}(T)$, increases monotonically, and diverges at $q = q_d(T)$, where $|j_s| = j_d(T)$. Because $\mathcal{L}_k(q,T)/\mathcal{L}_{k0}(T)$ diverges as $|j_s| \to j_d$, we show in Fig. 7 the typical dependence of the inverse $\mathcal{L}_{k0}(T)/\mathcal{L}_k(q,T) = 1/F_s[|j_s|/j_d(T)]$ versus $|j_s|/j_d(T)$. This figure was obtained by (a) evaluating $\tilde{j}_q(T)$ [Eq. (19)] and $d\tilde{j}_q(T)/dq$ numerically for $t = T/T_{c0} = 0$, 0.1, 0.2, 0.3, 0.4, 0.5, 0.6, 0.7, 0.8, and 0.9, and analytically [see Eq. (40)] in the GL limit $t \to 1$, (b) calculating

$$\frac{\mathcal{L}_{k0}(T)}{\mathcal{L}_k(q,T)} = \frac{n_{s0}(0)}{n_{s0}(T)} q_m(0) \frac{d\tilde{j}(T)}{dq} \tag{49}$$

using Eq. (14) to evaluate $n_{s0}(0)/n_{s0}(T)$, and (c) making a parametric plot of $\mathcal{L}_{k0}(T)/\mathcal{L}_k(q,T)$ versus $|j_s|/j_d = \tilde{j}_q(T)/\tilde{j}_d(T)$. As shown by the solid curve for $t = 0$, the dotted curve for $t = 0.3$, and the dashed curve for $t \to 1$, the behavior of $\mathcal{L}_{k0}(T)/\mathcal{L}_k(q,T)$ versus $|j_s|/j_d(T)$ is not monotonic as the temperature changes, but the curves for all other temperatures (not shown) lie in a narrow band between the dotted and dashed curves. As $|j_s|/j_d \to 1$, all the curves have an inverse-square-root dependence close to that in the GL limit $t \to 1$:

$$\mathcal{L}_{k0}^{\rm GL}(T)/\mathcal{L}_k^{\rm GL}(q,T) = (2\sqrt{6}/3)[1 - |j_s|/j_d(T)]^{1/2}. \tag{50}$$

The curves shown in Fig. 7 can be represented by $y_{sn}(x) = (1 - x^n)^{1/n}$ (not shown in Fig. 7), which fits the calculated values of $y = \mathcal{L}_{k0}(T)/\mathcal{L}_k(q,T)$ versus $x = |j_s|/j_d(T)$ for $0 \leqslant x < 0.97$ with 1% accuracy for $(n,t) = (2.21, 0)$, (2.21, 0.1), (2.27, 0.2), (2.30, 0.3), (2.28, 0.4), (2.25, 0.5), (2.22, 0.6), (2.18, 0.7), (2.16, 0.8), (2.13, 0.9), and $(2.11, t \to 1)$.

To calculate the kinetic inductivity in the GL limit shown by the dashed curve in Fig. 7, it is convenient to use the parametric relations $x = |j_s|/j_d = \sin\phi$ and $y = \mathcal{L}_{k0}^{\rm GL}(T)/\mathcal{L}_k^{\rm GL}(q,T) = 2\cos(2\phi/3) - 1$, where $0 \leqslant \phi \leqslant \pi/2$ [see Eqs. (45)–(47)]. The slow-experiment kinetic inductivity of the superfluid in the GL limit is

$$\mathcal{L}_k^{\rm GL}(q,T) = \mu_0\lambda_0^2(T) F_s^{\rm GL}\left(\frac{|j_s|}{j_d(T)}\right), \tag{51}$$

where

$$F_s^{\rm GL}(x) = \frac{1}{2\cos(2\phi/3) - 1} \tag{52}$$

and $\phi = \sin^{-1} x$. For small values of x,

$$F_s^{\rm GL}(x) = 1 + \tfrac{4}{9}x^2 + \tfrac{80}{243}x^4 + O(x^6), \tag{53}$$

and $F_s^{\rm GL}(x)$ diverges at $x = 1$, as noted in Ref. 13. (See also the upper solid curve in Fig. 10.)

IV. SUPERFLUID KINETIC INDUCTIVITY IN FAST EXPERIMENTS (SLOW RELAXATION)

We next consider fast experiments (or, equivalently, slow relaxation), in which the current density $j_s(t) = \bar{j}_s + j_{s1}(t)$ as a function of the time t changes rapidly about its time average $\bar{j}_s$ on a time scale $\tau_{\rm expt}$ much shorter than the relaxation time τ_s.[13,24,45] In this case, neither the order parameter Δ_q nor the q-dependent penetration depth λ_q can follow the time dependence of the current, but instead they remain frozen to their values at $q = \bar{q}$ given by $\bar{j}_s = j_{s\bar{q}} = -\bar{A}_s/\mu_0\lambda_{\bar{q}}^2$, where $\bar{A}_s = m\bar{v}_s/e = \hbar\bar{q}/2e$. From $j_s(t) = -A_s(t)/\mu_0\lambda_{\bar{q}}^2$, $A_s(t) = \bar{A}_s + A_{s1}(t)$, and $E(t) = -dA_s(t)/dt = \mathcal{L}_k(\bar{q},T)dj_s(t)/dt$, we find that the kinetic inductivity of the superfluid in fast experiments is

$$\mathcal{L}_k(\bar{q},T) = \mu_0\lambda_{\bar{q}}^2(T) = \mu_0\lambda_0^2(T) F_f\left(\frac{|\bar{j}_s|}{j_d(T)}\right), \tag{54}$$

which can be evaluated numerically using Eq. (16) as

$$\frac{\mathcal{L}_k(\bar{q},T)}{\mathcal{L}_{k0}(T)} = \frac{n_{s0}(T)}{n_{s\bar{q}}(T)} = \sum_{n=0}^{\infty} \frac{1}{1+u_{n0}^2} \Big/ \sum_{n=0}^{\infty} \frac{1}{1+u_{n\bar{q}}^2}. \tag{55}$$

(See Fig. 2.) Here, the fast-experiment function F_f is simply $\mathcal{L}_k(\bar{q},T)/\mu_0\lambda_0^2(T)$ but expressed as a function of the normalized current density $|\bar{j}_s|/j_d(T)$ rather than as a function of $\bar{q}$. When $\bar{q} \to 0$, $\mathcal{L}_k(\bar{q},T)$ reduces to $\mathcal{L}_k(0,T) = \mathcal{L}_{k0}(T)$ [Eq. (2)].

Shown in Fig. 8 is the typical dependence of $\mathcal{L}_k(\bar{q},T)/\mathcal{L}_{k0}(T)$ versus $|\bar{j}_s|/j_d(T)$. This figure was obtained by (a) evaluating $\tilde{j}_{\bar{q}}(T)$ and $\mathcal{L}_k(\bar{q},T)/\mathcal{L}_{k0}(T)$ numerically for $t = T/T_{c0} = 0$, 0.1, 0.2, 0.3, 0.4, 0.5, 0.6, 0.7, 0.8, and 0.9, and analytically in the GL limit $t \to 1$ [see Eqs. (45) and (47)], and (b) making a parametric plot of $\mathcal{L}_k(\bar{q},T)/\mathcal{L}_{k0}(T)$ versus $|\bar{j}_s|/j_d = \tilde{j}_{\bar{q}}(T)/\tilde{j}_d(T)$. As shown by the solid curve for $t = 0$, the dotted curve for $t = 0.3$, and the dashed curve for $t \to 1$, the behavior of $\mathcal{L}_k(\bar{q},T)/\mathcal{L}_{k0}(T)$ versus $|\bar{j}_s|/j_d$ is not monotonic as the temperature changes, but the curves for all other temperatures (not shown) lie in a narrow band between the dotted and dashed curves. As $|\bar{j}_s|/j_d \to 1$, all the curves approach their limiting values in the range 1.41–1.50 (solid symbols in Fig. 8) with infinite slope.

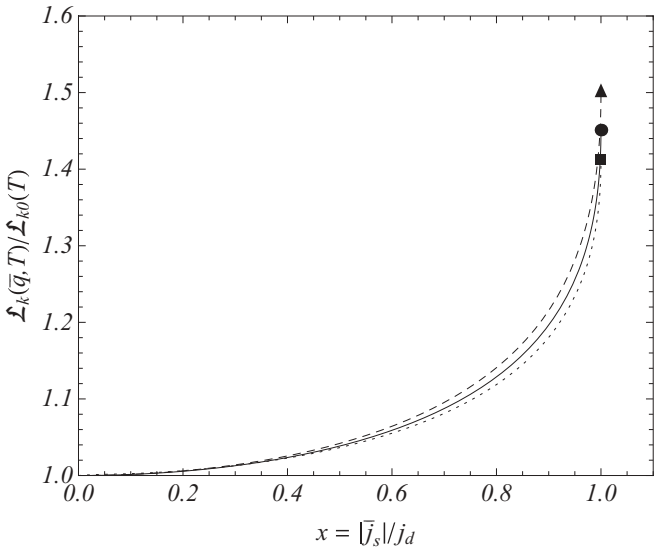

FIG. 8. $\mathcal{L}_k(\bar{q},T)/\mathcal{L}_{k0}(T) = F_f[|\bar{j}_s|/j_d(T)]$ for fast experiments vs $x = |\bar{j}_s|/j_d(T)$ at $t = T/T_{c0} = 0$ (solid curve and filled circle), $t = 0.3$ (dotted curve and filled square), and $t \to 1$ (dashed curve and filled triangle). Note that $\mathcal{L}_{k0}(T) = \mu_0\lambda_0^2(T)$.

The curves shown in Fig. 8 can be represented by $y_{fn}(x) = y_0 - (y_0 - 1)(1 - x^n)^{1/n}$ (not shown in Fig. 8), which fits the calculated values of $y = \mathcal{L}_k(\bar{q},T)/\mathcal{L}_{k0}(T)$ versus $x = |j_s|/j_d$, where y_0 is the value of $\mathcal{L}_k(\bar{q},T)/\mathcal{L}_{k0}(T)$ at $x = 1$, for $0 \leqslant x < 0.97$ within 0.5% for (y_0,n,t) = (1.451, 2.48, 0), (1.448, 2.47, 0.1), (1.422, 2.45, 0.2), (1.412, 2.46, 0.3), (1.417, 2.50, 0.4), (1.432, 2.50, 0.5), (1.448, 2.50, 0.6), (1.463, 2.50, 0.7), (1.477, 2.50, 0.8), (1.490, 2.50, 0.9), and (1.500, 2.50, $t \to 1$).

To calculate $\mathcal{L}_k(\bar{q},T)$ in the GL limit shown by the dashed curve in Fig. 8, we used Eqs. (45)–(47). The kinetic inductivity of the superfluid for fast experiments in the GL limit is

$$\mathcal{L}_k^{\rm GL}(\bar{q},T) = \mu_0\lambda_0^2(T)F_f^{\rm GL}\left(\frac{|\bar{j}_s|}{j_d}\right), \tag{56}$$

where

$$F_f^{\rm GL}(x) = \frac{1}{f^2(x)} = \frac{3}{1 + 2\cos(2\phi/3)} \tag{57}$$

and $\phi = \sin^{-1} x$. As noted in Ref. 13, for small values of x,

$$F_f^{\rm GL}(x) = 1 + \tfrac{4}{27}x^2 + \tfrac{16}{243}x^4 + O(x^6), \tag{58}$$

and $F_f^{\rm GL}(x)$ approaches 3/2 with infinite slope as $x \to 1$. (See also the lower solid curve in Fig. 10.)

V. KINETIC IMPEDIVITY OF THE SUPERFLUID $\mathcal{Z}_{ks}$

In the above sections, we discussed the situations when $\tau_{\rm expt}/\tau_s$ is large or small. To describe in detail the transition between these two limits is well beyond the scope of this paper, because this topic involves nonequilibrium processes with numerous relaxation times.[24,45,46] We present here a simplified procedure for approximating the transition between the two limits, which may prove instrumental in analysis of experimental data.

For the moment, we restrict our attention to the GL regime and employ a phenomenological model assuming that the time dependence of f is determined by simplest version of the time-dependent GL (TDGL) equation,[24]

$$\tau_s df/dt = f - f^3 - A_s'^2 f, \tag{59}$$

where $A_s' = A_s/(\phi_0/2\pi\xi)$. An important caution here is that we are using this equation in the gapped state, even though a nonlinear TDGL equation has been rigorously justified only in a gapless superconductor,[57] where near T_c and at frequencies $\omega\tau_s \ll 1$, $\tau_s = \pi\hbar/8k_B(T_c - T)$.[24]

In the GL regime $[(T_c - T) \ll T_c]$, the supercurrent density [Eq. (18)] becomes in dimensionless quantities

$$j_s' = -f^2 A_s', \tag{60}$$

where $j_s' = j_s/(\phi_0/2\pi\mu_0\xi\lambda_0^2)$. We now consider experiments in which the dimensionless supercurrent density $j_s'(t)$ as a function of the time t changes about its time average on a time scale $\tau_{\rm expt}$ comparable with the relaxation time τ_s. In particular, we consider the linear response of the superconducting strip to a time-dependent supercurrent density given by $j_s'(t) = j_{s0}' + j_{s1}'e^{i\omega t}$, where j_{s0}', the bias current current density, is fixed to be in the range $0 \leqslant |j_{s0}'| < j_d'$, and j_{s1}', the amplitude of the ac current density, obeys $j_{s1}' \ll j_{s0}'$. In this section, we assume that the frequencies are sufficiently low that normal-fluid currents are not excited such that the current is all supercurrent. To analyze the linear response of the reduced order parameter to the ac current, we substitute $j_s' = j_{s0}' + j_{s1}'e^{i\omega t}$ and $f = f_0 + f_1 e^{i\omega t}$ $(|f_1| \ll f_0)$ into Eq. (59), where f_0 $(\sqrt{2/3} \leqslant f_0 \leqslant 1)$ is the solution of Eq. (59) in the time-independent case when $j_s' = j_{s0}'$. We then linearize Eq. (59) by neglecting terms of order $\tilde{j}_{s1}^2$ and f_1^2. The solution is

$$f_1 = -\frac{2j_{s0}'j_{s1}'}{f_0^3\left(6f_0^2 - 4 + i\omega\tau_s\right)}. \tag{61}$$

(Note that this result is obtained for sinusoidal variation of the supercurrent around a fixed value of j_{s0}'. A different result would be obtained for sinusoidal variation of the gauge-invariant vector potential around a fixed value of A_{s0}'.)

From $E = -dA_s/dt$, Eq. (60), and $j_{s0}'^2 = f_0^4(1 - f_0^2)$ we obtain the electric field in the linear-response approximation:

$$E = \mu_0\lambda_0^2\left(\frac{2f_0^2 + i\omega\tau_s}{f_0^2\left(6f_0^2 - 4 + i\omega\tau_s\right)}\right)\frac{dj_{s1}}{dt} \tag{62}$$

$$= \mathcal{Z}_{ks}j_{s1} = (\mathcal{R}_{ks} + i\mathcal{X}_{ks})j_{s1} \tag{63}$$

$$= (\mathcal{R}_{ks} + i\omega\mathcal{L}_k)j_{s1}. \tag{64}$$

The coefficient of dj_{s1}/dt on the right-hand side of Eq. (62) reduces to the slow-experiment inductivity $\mathcal{L}_k^{\rm GL}(q,T)$ [Eq. (51)] in the limit $\omega\tau_s \to 0$ and to the fast-experiment inductivity $\mathcal{L}_k^{\rm GL}(\bar{q},T)$ [Eq. (56)] in the limit $\omega\tau_s \to \infty$.

The complex kinetic impedivity (specific impedance or complex resistivity) of the superfluid $\mathcal{Z}_{ks}$, here evaluated in the GL regime, can be conveniently expressed in terms of $F_s^{\rm GL}$ [Eq. (52)] and $F_f^{\rm GL}$ [Eq. (57)] as

$$\mathcal{Z}_{ks} = i\omega\mu_0\lambda_0^2\left(\frac{F_s^{\rm GL} + F_f^{\rm GL}i\omega\tau_{\rm eff}}{1 + i\omega\tau_{\rm eff}}\right), \tag{65}$$

where

$$\tau_{\rm eff} = F_s^{\rm GL}\tau_s/2. \tag{66}$$

(For a long strip of length ℓ, width W, and thickness d, the complex kinetic impedance is $Z_{ks} = \mathcal{Z}_{ks}\ell/Wd$.)

The real part $\mathcal{R}_{ks}$ of the superfluid kinetic impedivity is the frequency-dependent resistivity of the superfluid due to order-parameter relaxation. Using the the parametric relation $x = |j_{s0}|/j_d = \sin\phi$ as above, we obtain

$$\mathcal{R}_{ks} = \frac{\mu_0\lambda_0^2}{\tau_s}G\left(\frac{|j_{s0}|}{j_d},\omega\tau_s\right), \tag{67}$$

$$G(x,\omega\tau_s) = \frac{\beta(\phi)(\omega\tau_s)^2}{\alpha^2(\phi)+(\omega\tau_s)^2}, \tag{68}$$

$$\alpha(\phi) = 4\cos(2\phi/3) - 2, \tag{69}$$

$$\beta(\phi) = \frac{16\sin^2(\phi/3)}{1+2\cos(2\phi/3)}. \tag{70}$$

$G(x,\omega\tau_s)$ is shown in Fig. 9 as a function of x for various values of $\omega\tau_s$. In limiting cases, we have

$$G(x,\omega\tau_s) = \frac{16}{27}x^2 + \frac{64}{243}x^4 + O(x^6), \quad \omega\tau_s \gg 1 \tag{71}$$

$$= \left[\frac{4}{27}x^2 + \frac{16}{81}x^4 + O(x^6)\right](\omega\tau_s)^2, \quad \omega\tau_s \ll 1 \tag{72}$$

and $G(x,\omega\tau_s)$ approaches 2 with infinite slope as $x \to 1$.

Although the superconducting strip has zero dc electrical resistivity, under ac conditions order-parameter relaxation contributes to dissipation of energy in a manner similar to the way it contributes to flux-flow dissipation.[24,58–61] The time-averaged rate of energy dissipation per unit volume via order-parameter relaxation is $(1/2)\mathcal{R}_{ks}j_{s1}^2$, which also can be calculated using the dissipation function discussed in Refs. 59 and 60.

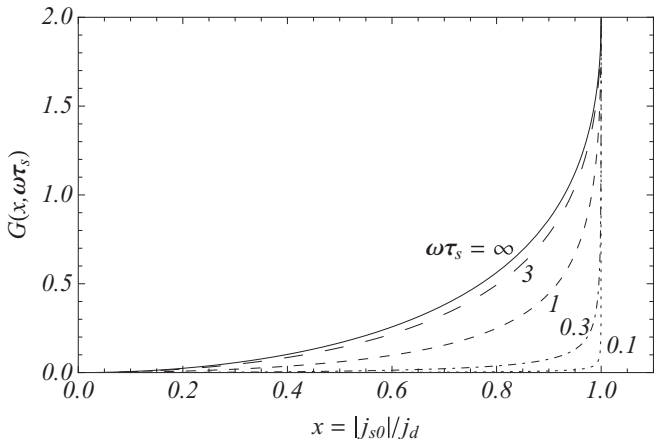

FIG. 9. $G(x,\omega\tau_s)$, which describes the alternating-current resistivity of the superfluid due to order-parameter relaxation [Eqs. (67) and (68)], vs $x = |j_{s0}|/j_d$ for $\omega\tau_s = 0.1$ (dotted line), $\omega\tau_s = 0.3$ (dotted-dashed line), $\omega\tau_s = 1$ (dashed line), $\omega\tau_s = 3$ (long dashed line), and $\omega\tau_s = \infty$. $G(1,\omega\tau_s) = 2$.

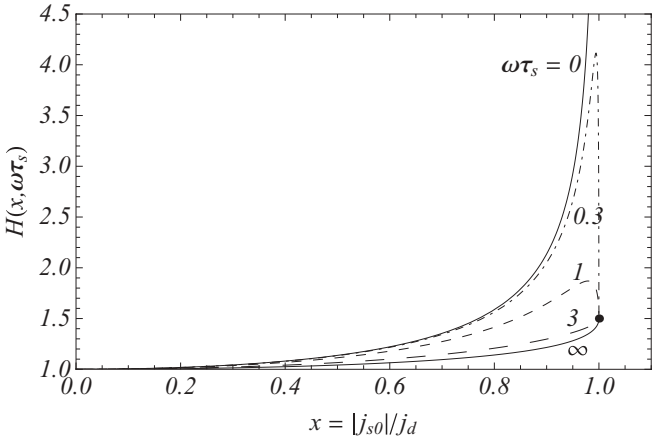

FIG. 10. $H(x,\omega\tau_s)$, which describes the superfluid's kinetic inductivity [Eqs. (73) and (74)], vs $x = |j_{s0}|/j_d$ for $\omega\tau_s = 0$ [upper solid curve, for which $H(x,0) = F_s^{\rm GL}(x)$, Eq. (52)], $\omega\tau_s = 0.3$ (dotted-dashed line), $\omega\tau_s = 1$ (dashed line), $\omega\tau_s = 3$ (long dashed line), and $\omega\tau_s = \infty$ [lower solid curve, for which $H(x,0) = F_f^{\rm GL}(x)$, Eq. (57)]. For nonzero $\omega\tau_s$, $H(1,\omega\tau_s) = 1.5$ (black point).

The superfluid's kinetic reactivity is $\mathcal{X}_{ks} = \omega\mathcal{L}_k$, where the superfluid's kinetic inductivity $\mathcal{L}_k$ is

$$\mathcal{L}_k = \mu_0\lambda_0^2 H\left(\frac{|j_{s0}|}{j_d},\omega\tau_s\right), \tag{73}$$

$$H(x,\omega\tau_s) = \frac{1}{1+2\cos(2\phi/3)}\left[3 + \frac{16\alpha(\phi)\sin^2(\phi/3)}{\alpha^2(\phi)+(\omega\tau_s)^2}\right]. \tag{74}$$

Shown in Fig. 10 are plots of $H(x,\omega\tau_s)$ versus x for various values of $\omega\tau_s$. As expected, $H(x,\omega\tau_s)$ approaches the slow-experiment result $F_s^{\rm GL}(x)$ when $\omega\tau_s \to 0$ and the fast-experiment result $F_f^{\rm GL}(x)$ as $\omega\tau_s \to \infty$.

In the above, we have used the relatively simple formalism of the time-dependent GL theory, bearing in mind that there are questions of whether this theory can legitimately be used for gapped superconductors and how τ_s can be determined. A reasonable starting point for an approximate phenomenological theory of the complex kinetic impedivity of the superfluid $\mathcal{Z}_{ks}$ at lower temperatures outside the GL regime would be to replace the quantities $F_s^{\rm GL}$ and $F_f^{\rm GL}$ in Eqs. (65) and (66) by the more general expressions F_s and F_f given in Eqs. (48) and (54). Note from Figs. 7 and 8 that $F_s = \mathcal{L}_k(q,T)/\mu_0\lambda_0^2(T)$ and $F_f = \mathcal{L}_k(\bar{q},T)/\mu_0\lambda_0^2(T)$ as functions of $|j_s|/j_d$ and $|j_s|/j_d$ do not differ greatly from their GL counterparts $F_s^{\rm GL}$ and $F_f^{\rm GL}$. Although the theory we have presented here is not rigorous, our results suggest that when $\omega\tau_s \gg 1$ but when ω is well below the superconducting gap frequency $2\Delta_q(T)/\hbar$, order-parameter relaxation gives rise to a current- and frequency-dependent contribution to the ac resistivity separate from that due to the normal fluid (thermally excited quasiparticles). However, as discussed above, remaining unknown is how to calculate order-parameter relaxation and how to determine the relaxation times that should replace τ_s in a more complete theory.[45]

VI. KINETIC IMPEDANCE INCLUDING THE NORMAL-FLUID RESPONSE

We examine next the current dependence of the dissipation arising from the flow of thermally excited quasiparticles at frequencies ω well below the superconducting gap frequency $2\Delta_q(T)/\hbar$. This is the frequency regime where a two-fluid approach is generally applicable.[24] However, the two-fluid terminology needs to be used with caution because, as explained below, coherence-factor effects can produce dissipation greater than in the normal state.[62] Although the quasiparticles have their own kinetic inductivity,[5] their reactive contribution to the total kinetic impedivity is negligible at the frequencies of interest here. The quasiparticles' only significant contribution to the ac normal-fluid current density is therefore

$$j_{n1} = \sigma_1 E, \tag{75}$$

where σ_1 corresponds to the real part of the complex conductivity $\sigma = \sigma_1 - i\sigma_2$, the linear-response function connecting $\boldsymbol{j}$ and $\boldsymbol{E}$ calculated by Mattis and Bardeen.[63]

We begin by reexpressing σ_1 for the BCS case as[64]

$$\sigma_1 = \frac{\sigma_n}{\omega}\int_{-\infty}^{\infty} d\omega' \left[f\left(\omega' - \frac{\omega}{2}\right) - f\left(\omega' + \frac{\omega}{2}\right)\right] \times \left[n_1\left(\omega' - \frac{\omega}{2}\right) n_1\left(\omega' + \frac{\omega}{2}\right) + p_1\left(\omega' - \frac{\omega}{2}\right) p_1\left(\omega' + \frac{\omega}{2}\right)\right], \tag{76}$$

where ω is expressed in energy units ($\hbar = 1$) and $f(\omega) = 1/(1 + e^{\beta\omega})$ is the Fermi function. For the BCS case,

$$n_1(\omega) = \mathrm{Re}\frac{\omega}{\sqrt{\omega^2 - \Delta^2}}, \tag{77}$$

$$p_1(\omega) = \mathrm{Re}\frac{\Delta}{\sqrt{\omega^2 - \Delta^2}}, \tag{78}$$

$n_1(\omega) = p_1(\omega) = 0$ for $|\omega| < \Delta(T)$, and the signs of the square roots are chosen such that $n_1(\omega)$ is an even function and $p_1(\omega)$ an odd function of ω. At $T = 0$, the Fermi functions freeze-out all contributions to σ_1 for $\omega < 2\Delta(0)$, such that σ_1 is nonvanishing only for $\omega > 2\Delta(0)$, when the integral of Eq. (76) can be expressed in terms of complete elliptic integrals.[24,63] For $T > 0$ and frequencies obeying $\omega \ll 2\Delta(0)$, σ_1/σ_n plotted as a function of temperature is found theoretically in dirty superconductors[62] to be very small at low temperatures, rising to a maximum at which $\sigma_1/\sigma_n > 1$ [for example,[62] $\sigma_{1\max}/\sigma_n = 2.17$ at $t = 0.864$ when $\omega/\Delta(0) = 0.02$] and returning to 1 at $t = T/T_{c0} = 1$. A similar temperature dependence has been seen experimentally in several materials.[65–68]

Because the coherence-factor terms n_1 and p_1 in Eq. (76) yield a logarithmic divergence for $\omega = 0$, σ_1 can be evaluated approximately at low temperatures [$\Delta(T)/k_BT \gtrsim 2$] and low frequencies [$\omega \ll 2\Delta(0)$] by introducing a cutoff energy $\epsilon \sim \omega$. The leading term in the result is

$$\sigma_1 \approx 2\sigma_n \left[\frac{\Delta(T)}{k_BT}\right] \exp\left[-\frac{\Delta(T)}{k_BT}\right] \ln\left(\frac{k_BT}{\epsilon}\right). \tag{79}$$

The expressions for σ_1 derived by Nam[34–36] for strong-coupling superconductors also can be put into the form of Eq. (76), except that Δ in Eqs. (77) and (78) must then be replaced by the complex gap function $\Delta(\omega)$, which contains additional phonon-related ω dependence due to the electron-phonon interaction.[69]

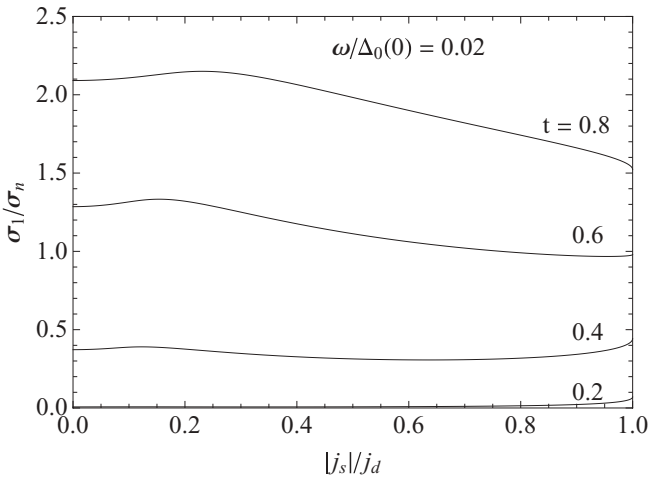

FIG. 11. σ_1/σ_n vs $|j_s|/j_d$ calculated from Eqs. (76), (80), and (81) for $\omega/\Delta_0(0) = 0.02$ and $t = T/T_{c0} = 0.2$, 0.4, 0.6, and 0.8.

For the pair-breaking theory of superconductors with paramagnetic impurities[32–36] or, as in the case of interest here, current-carrying thin films,[27–29,31,37,70,71] Eqs. (77) and (78) are replaced by

$$n_1(\omega) = \mathrm{Re}\frac{u}{\sqrt{u^2 - 1}}, \tag{80}$$

$$p_1(\omega) = \mathrm{Re}\frac{1}{\sqrt{u^2 - 1}}, \tag{81}$$

where u is given by Eq. (D3), $n_1(\omega) = p_1(\omega) = 0$ for $|\omega| < \omega_g$ with[32] $\omega_g/\Delta_q = (1 - \zeta^{2/3})^{3/2}$, and the signs of the square roots are chosen such that $n_1(\omega)$ is an even function and $p_1(\omega)$ an odd function of ω. (See, for example, Fig. 4 in Ref. 32 or Fig. 6 in Ref. 33.) Numerical evaluation of Eq. (76) using Eqs. (80) and (81) in the limit as $\zeta \to 0$ yield $\sigma_1(\omega)$ values in agreement with the dirty-limit Mattis-Bardeen results.[24,63]

Figure 11 shows σ_1/σ_n versus $|j_s|/j_d$ for $\omega/\Delta_0(0) = 0.02$ and several values of $t = T/T_{c0}$. σ_1/σ_n was first calculated from Eq. (76) as a function of $q/q_m(0)$ up to $q_d(T)/q_m(0)$, accounting for the q and temperature dependence of $\zeta = (q^2/2q_m^2)\Delta_0(0)/\Delta_q(T)$. (See Fig. 1.) Figure 11 was then constructed as a parametric plot using $|j_s|/j_d$ versus $q/q_m(0)$ up to $q_d(T)/q_m(0)$ obtained as in Fig. 3. The main features of the dependence of σ_1/σ_n can be understood from Eq. (79), but where $\Delta(T)$ is replaced by $\Delta_q(T)$ (see Fig. 1) and the cutoff ϵ is replaced by the larger of $\epsilon_\omega \sim \omega$ or the peak width in $n_1(\omega)$, $\epsilon_\zeta \sim \Delta_q - \omega_g \approx (3/2)\Delta_q\zeta^{2/3}$. The exponential term in Eq. (79) tends to make σ_1 increase as q and $|j_s|$ (see Figs. 3 and 6) increase, as seen in Fig. 11 for small values of $|j_s|/j_d$, where $\epsilon_\omega > \epsilon_\zeta$ and the $\ln(k_BT/\epsilon_\omega)$ term is a constant. Maxima occur when $\epsilon_\omega \approx \epsilon_\zeta$. To the right of the maxima, $\epsilon_\zeta > \epsilon_\omega$, and the term $\ln(k_BT/\epsilon_\zeta)$, which is a decreasing function of q and $|j_s|$, plays a stronger role.

The current density carried by the normal fluid, accounting for the effects of the coherence factor, is given by Eq. (75). We also can express the normal-fluid response in terms of the normal fluid's kinetic impedivity $\mathcal{Z}_{kn} = 1/\sigma_1$. Because the

total ac current density carried by the strip is $j_1 = j_{s1} + j_{n1}$, and $E = \mathcal{Z}_k j_{s1}$, the overall kinetic impedivity $\mathcal{Z}_k = \mathcal{R}_k + i\mathcal{X}_k = \mathcal{R}_k + i\omega\mathcal{L}_k$ of the strip, including the normal-fluid response, is the impedances-in-parallel combination

$$\mathcal{Z}_k = \left(\mathcal{Z}_{ks}^{-1} + \mathcal{Z}_{kn}^{-1}\right)^{-1}. \tag{82}$$

Note that as $T \to T_{cq}$, $|\mathcal{Z}_{ks}|$ diverges, $\mathcal{Z}_{kn} \to 1/\sigma_n$, and $\mathcal{Z}_k$ approaches the normal-state resistivity.

In the limit as $j_{s0} \to 0$, our results reduce to the well-known two-fluid description[24] when the impedivity can be expressed in terms of the complex conductivity $\sigma = \sigma_1 - i\sigma_2$, the linear-response function connecting $\boldsymbol{j}$ and $\boldsymbol{E}$ calculated by Mattis and Bardeen.[63] As $\boldsymbol{j}_{s0} \to 0$, $\mathcal{R}_{ks} \to 0$, $\mathcal{X}_{ks} \to \omega\mathcal{L}_{ks} = \mu_0\omega\lambda_0^2 = 1/\sigma_2$, $\sigma_{nf} \to \sigma_1$, $\mathcal{Z}_{ks} \to i/\sigma_2$, $\mathcal{Z}_{kn} \to 1/\sigma_1$, and $\mathcal{Z}_k \to (\sigma_1 - i\sigma_2)^{-1} = \sigma^{-1}$.

At temperatures above T_{cq}, the normal-state impedance is $Z = R_n + i\omega(L_k + L_m)$, where L_m is the geometric inductance associated with stored magnetic energy and, for a long strip of conduction-electron density n_c, total length ℓ, width W, and thickness d, $L_k = (m/n_c e^2)(\ell/Wd)$ is the normal-state kinetic inductance.[5] The impedance is usually dominated by the normal-state resistance $R_n = \rho_n \ell/Wd$ except at very high frequencies.[5]

VII. DISCUSSION

In this paper, we have presented fundamental theoretical calculations of the kinetic impedance of thin and narrow impure superconducting films for all temperatures and for all currents up to the depairing current. Our results should be applicable to ongoing experimental studies of small-scale superconducting devices in which the kinetic inductance plays an important role. Our calculations have shown examples of how the kinetic inductance and the normal-fluid dissipation depend upon the dc applied current. However, experiments examining the in-phase and out-of-phase third and higher harmonics might provide a more sensitive means of revealing the influence of the nonlinearities implied by these current dependencies.[72]

Our results in the GL regime for the bias-current dependence of the kinetic inductance are in agreement with those of Anlage *et al.*[13] and Annunziata *et al.*[2] for the slow-experiment case and with the result of Anlage *et al.*[13] for the fast-experiment case. However, Annunziata *et al.*,[2] in examining the case of $T = 0$ and noting correctly that $\lambda_0^2(0)$ is inversely proportional to $\Delta_0(0)$ (in our notation) [see Eq. (B3)], assumed that $\lambda_q^2(0)$ is inversely proportional to $\Delta_q(0)$. This assumption is incorrect, as can be seen from Eqs. (23), (26), and (28). As a consequence, their prediction for the current dependence of the kinetic inductance does not agree with our results for either slow or fast experiments.

In practice, the depairing current density might be smaller than calculated here for a number of reasons. In thin and narrow strips with sharp corners, current crowding leads to suppression of the order parameter in the immediate vicinity of sharp inner corners, and this can cause the critical current in such devices to be considerably lower than the depairing value.[19,23,73–76] By optimally rounding the inner corners, one should be able to raise the critical current to values close to the depairing value.[19,23,75]

As discussed in Sec. II, our calculation of the critical depairing-current density j_d has been carried out within a mean-field approach disregarding fluctuations. However, the experimental critical current density j_c could be somewhat smaller than j_d as a result of thermal or quantum fluctuations, which can initiate phase slips in one-dimensional (1D) wires[77,78] or vortex nucleation at the edges of strips[15,16,23,79] when an energy barrier is overcome or suppressed to zero. The fluctuation limited j_c therefore may prevent the observation of both the predicted divergence of the slow-experiment kinetic inductivity at j_d and the approach to the maximum values of the fast-experiment kinetic inductivity (shown by the filled symbols in Fig. 8). In fact, previous experimental observations of a relatively small kinetic inductance rising to a peak and then rapidly dropping to smaller values with increasing applied current[2,14,80,81] are explainable in terms of the growth of high-resistance normal regions as the current density rises above j_c.

As discussed in Secs. III–V, relaxation of the superfluid, approximately characterized here by the relaxation time τ_s, plays an important role in determining both the real and imaginary parts of the kinetic impedance. To examine the physics of relaxation dynamics is beyond the scope of this paper, and for further discussion we refer the reader to Refs. 24 and 45 and references therein. Nevertheless, Figs. 9 and 10 suggest means by which τ_s could be estimated from experimental determinations of the superfluid's ac resistivity and inductivity. At the very least, such experiments should be able to reveal whether they are in the slow- or fast-experiment limit, and experiments carried out at different frequencies and temperatures might be able to show the transition between these two limits.

In this paper, we have used the concept of the q-dependent penetration depth, which increases as the current density increases. This occurs because an increase of the current density causes a decrease in the magnitude of the superconducting order parameter. This concept is the basis of the effective field-dependent penetration depth in type-II superconductors $\lambda(B,T)$, which diverges as $B \to B_{c2}(T)$. This quantity has been introduced to understand such phenomena as small-angle neutron-scattering form factors,[82] magnetic coupling of vortex lattices in dc superconducting transformers,[83,84] magnetization curves in low-pinning superconductors,[85] elastic properties of the vortex lattice,[86] and μSR measurements in the mixed state.[87,88]

ACKNOWLEDGMENTS

We thank K. K. Berggren, Y. Mawatari, D. Prober, D. Santavicca, and S. M. Anlage for stimulating suggestions and comments. This research was supported by the US Department of Energy, Office of Basic Energy Science, Division of Materials Sciences and Engineering and was performed at the Ames Laboratory, which is operated for the US Department of Energy by Iowa State University under Contract No. DE-AC02-07CH11358.

APPENDIX A: u_{nq}

The function $u_{nq}(\eta,\epsilon,\zeta)$ is the solution of the quartic equation

$$\epsilon^2 u^4 - 2\eta\epsilon u^3 + (\eta^2 + \epsilon^2 - \epsilon^2\zeta^2)u^2 - 2\eta\epsilon u - \eta^2 = 0, \tag{A1}$$

obtained from Eq. (9). The desired solution of the quartic equation is

$$u_{nq} = (f + g + \eta/\epsilon)/2, \tag{A2}$$

where

$$a = -2[\epsilon^6(\zeta^2-1)^3 - 3\epsilon^4(1+16\zeta^2+\zeta^4)\eta^2 + 3\epsilon^2(\zeta^2-1)\eta^4 - \eta^6], \tag{A3}$$

$$b = \sqrt{-4c^6 + a^2}, \tag{A4}$$

$$c = \epsilon^2(\zeta^2-1) - \eta^2, \tag{A5}$$

$$d = (a+b)^{1/3}, \tag{A6}$$

$$e = \frac{2^{2/3}c^2 + d^2}{2^{1/3}3\epsilon^2 d}, \tag{A7}$$

$$f = \sqrt{\frac{2\epsilon^2(\zeta^2-1)+\eta^2}{3\epsilon^2} + e}, \tag{A8}$$

$$g = \sqrt{\frac{2[2\epsilon^2(\zeta^2-1)+\eta^2]}{3\epsilon^2} - e + \frac{2(\zeta^2+1)\eta}{\epsilon f}}. \tag{A9}$$

Similar solutions of the quartic equation that arises in the closely related problem of the density of states in the Abrikosov-Gor'kov theory[30] were obtained in Refs. 35 and 89.

APPENDIX B: ZERO-CURRENT LIMIT

In the limit of zero current, $q \to 0$ ($v_s \to 0$), $u_{n0} = \eta/\epsilon$, and we obtain from Eq. (11), after defining $t = T/T_{c0}$ and $\delta_0(T) = \Delta_0(T)/2\pi k_B T_{c0}$,

$$\ln\frac{1}{t} = \sum_{n=0}^{\infty}\left(\frac{1}{n+1/2} - \frac{1}{\sqrt{(n+1/2)^2 + \delta_0^2(T)/t^2}}\right), \tag{B1}$$

which yields the temperature dependence of $\Delta_0(T)$ for all temperatures between 0 and T_{c0}, the transition temperature for $q = 0$. An analysis of this equation as $t \to 0$ reveals that $4\pi\delta_0(0) = 2\Delta_0(0)/k_B T_{c0} = 2\pi e^{-\gamma} = 3.528$, which is consistent with the fact that the above form of the Usadel theory coincides with the weak-coupling BCS theory for an s-wave isotropic gap on a spherical Fermi surface. Values of $\Delta_0(T)/\Delta_0(0)$ versus $t = T/T_{c0}$, which reproduce well-known results,[50,90] can be obtained by numerically carrying out the sum in Eq. (B1), and it can be shown analytically that $[\Delta_0(T)/\Delta_0(0)]^2 \to [8e^{2\gamma}/7\zeta(3)](1-t) = 3.016(1-t)$ as $t \to 1$.

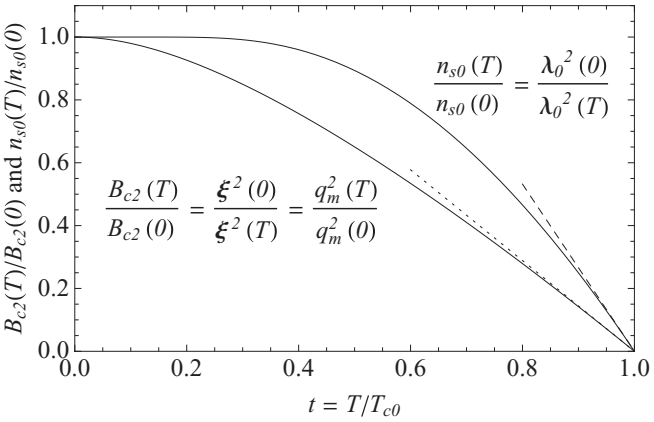

FIG. 12. Upper curve: reduced superfluid density $n_{s0}(T)/n_{s0}(0) = [\lambda_0(0)/\lambda_0(T)]^2$ vs $t = T/T_{c0}$, obtained from Eq. (14). The dashed line $2.660(1-t)$ shows the slope as $t \to 1$. Lower curve: reduced upper critical field $B_{c2}(T)/B_{c2}(0) = [\xi(0)/\xi(T)]^2$ vs $t = T/T_{c0}$, obtained from Eqs. (C9) and (C10). The dotted line $1.444(1-t)$ shows the slope as $t \to 1$.

In the zero-q limit, the sum in Eq. (16) can be evaluated analytically as shown in Eq. (14), such that, as previously discussed in Refs. 91 and 24,

$$\frac{n_{s0}(T)}{n_{s0}(0)} = \frac{\lambda_0^2(0)}{\lambda_0^2(T)} = \frac{\Delta_0(T)}{\Delta_0(0)}\tanh\left[\frac{\Delta_0(T)}{2k_B T}\right]. \tag{B2}$$

From Eq. (2), $\xi_0 = \hbar v_F/\pi\Delta_0(0)$, and the normal-state conductivity $\sigma_n = 2e^2 N(0)D$, we obtain

$$\frac{1}{\mu_0\lambda_0^2(T)} = \frac{n_{s0}(T)e^2}{m} = \frac{\pi\sigma_n\Delta_0(T)}{\hbar}\tanh\left[\frac{\Delta_0(T)}{2k_B T}\right]. \tag{B3}$$

Figure 12 exhibits the temperature dependence of $n_{s0}(T)$. As $t \to 1$, $n_{s0}(T)/n_{s0}(0) \to [4\pi e^{\gamma}/7\zeta(3)](1-t) = 2.660(1-t)$.

At $T = 0$, we can write

$$\frac{1}{\mu_0\lambda_0^2(0)} = \frac{2}{3}N(0)e^2 v_F^2\left(\frac{\ell}{\xi_0}\right), \tag{B4}$$

but because the zero-temperature London penetration depth $\lambda_L(0)$ can be expressed as[50]

$$\frac{1}{\mu_0\lambda_L^2(0)} = \frac{2}{3}N(0)e^2 v_F^2, \tag{B5}$$

we see that $\lambda_0(0) = \lambda_L(0)(\xi_0/\ell)^{1/2}$. (Recall that $\ell \ll \xi_0$ in the dirty limit under consideration here.)

APPENDIX C: ZERO-GAP LIMIT

To find the boundary in the t-q plane where $\Delta_q(T)$ is reduced to zero, note from Eq. (9) that $\epsilon\sqrt{1+u_{nq}^2} \to n + 1/2 + Q/2\pi k_B T$ in the limit $\epsilon = \Delta_q(T)/2\pi k_B T \to 0$, such that Eq. (11) then yields the q-dependent transition temperature. Defining $t_{cq} = T_{cq}/T_{c0}$,

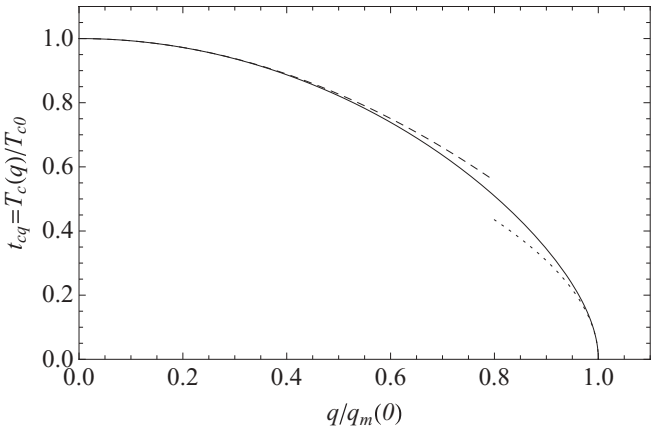

FIG. 13. $t_{cq} = T_{cq}/T_{c0}$ (solid) vs $q/q_m(0)$ obtained from Eqs. (23)–(25). Also shown are expansions of t_{cq} about $q = 0$ [dashed line, Eq. (C3)] and $q = q_m(0)$ [dotted line, Eq. (C4)]. This figure is the same as a plot of $t = T/T_{c0}$ along the ordinate vs $q_m(T)/q_m(0)$ along the abscissa. $\Delta_q(T) > 0$ only for values of t and $q/q_m(0)$ under the curve.

$P = Q/2\pi k_B T_{c0}$, $P_m = Q_m/2\pi k_B T_{c0} = e^{\psi(1/2)} = e^{-\gamma}/4 = 0.140$, $Q_m = \pi k_B T_{c0} e^{-\gamma}/2 = \hbar D q_m^2(0)/2$, $q_m(0) = (\pi k_B T_{c0} e^{-\gamma}/\hbar D)^{1/2} = (3/\pi\xi_0\ell)^{1/2}$, and $v_m(0) = (\hbar/2m)(\pi k_B T_{c0} e^{-\gamma}/\hbar D)^{1/2}$, we obtain

$$\ln\frac{1}{t_{cq}} = \sum_{n=0}^{\infty}\left(\frac{1}{n+1/2} - \frac{1}{n+1/2+P/t_{cq}}\right) \quad \text{(C1)}$$

$$= \psi\left(\frac{1}{2}+\frac{P}{t_{cq}}\right) - \psi\left(\frac{1}{2}\right), \quad \text{(C2)}$$

where ψ is the digamma function and $P/P_m = [q/q_m(0)]^2 = [v_s/v_m(0)]^2$. Figure 13 shows t_{cq} as a function of $q/q_m(0) = v_s/v_m(0)$. Expansions of t_{cq} about $q = 0$ and $q = q_m(0)$ yield, respectively, the approximations

$$t_{cq} = 1 - \frac{\pi^2 e^{-\gamma}}{8}\frac{q^2}{q_m^2(0)} = 1 - 0.693\frac{q^2}{q_m^2(0)} \quad \text{(C3)}$$

$$= \sqrt{3}e^{-\gamma}\sqrt{1-\frac{q}{q_m(0)}} = 0.972\sqrt{1-\frac{q}{q_m(0)}}, \quad \text{(C4)}$$

which are shown as the dashed and dotted curves in Fig. 13.

A similar procedure can be used to determine $q_m(T)$, the value of q that drives $\Delta_q(T)$ to zero for a given value of t. Equation (11) then yields

$$\ln\frac{1}{t} = \sum_{n=0}^{\infty}\left(\frac{1}{n+1/2} - \frac{1}{n+1/2+\alpha}\right) \quad \text{(C5)}$$

$$= \psi\left(\frac{1}{2}+\alpha\right) - \psi\left(\frac{1}{2}\right), \quad \text{(C6)}$$

where α is given in Eq. (34). Since t_{cq} and $q_m(T)$ are both determined by the equation obtained by setting $\Delta_q(T) = 0$, it should not be surprising that a plot of t versus $q_m(T)/q_m(0)$ is exactly the same as the plot of t_{cq} versus $q/q_m(0)$, shown in Fig. 13. Expansions of $q_m(T)/q_m(0)$ about $t = 0$ and 1 yield, respectively, the approximations

$$\frac{q_m(T)}{q_m(0)} = 1 - \frac{e^{2\gamma}}{3}t^2 = 1 - 1.057t^2 \quad \text{(C7)}$$

$$= \sqrt{\frac{8e^{\gamma}}{\pi^2}}e^{-\gamma}\sqrt{1-t} = 1.202\sqrt{1-t}, \quad \text{(C8)}$$

which correspond to the dotted and dashed curves in Fig. 13. Equations (C7) and (C8) are most easily obtained by making the replacements $q \to q_m(T)$ and $t_{cq} \to t$ in Eqs. (C3) and (C4).

The upper critical field is related to the temperature-dependent coherence length via $B_{c2}(T) = \phi_0/2\pi\xi^2(T)$, and, as discussed in Ref. 92, in the dirty limit B_{c2} can be obtained from the equation

$$\ln\left(\frac{1}{t}\right) = \psi\left(\frac{1}{2}+\rho\right) - \psi\left(\frac{1}{2}\right), \quad \text{(C9)}$$

where $t = T/T_{c0}$ and

$$\rho = \left(\frac{e^{-\gamma}}{4}\right)\left(\frac{B_{c2}(T)}{B_{c2}(0)}\right)\frac{1}{t}, \quad \text{(C10)}$$

where $B_{c2}(0) = \phi_0/2\pi\xi^2(0)$ and $\xi(0) = (\pi\xi_0\ell/3)^{1/2}$. At $t = 0$, we have $\lambda_0(0)/\xi(0) = \sqrt{3/\pi}\lambda_L(0)/\ell = 0.977\lambda_L(0)/\ell$.

As $t \to 0$, $B_{c2}(T)/B_{c2}(0) \approx 1 - (2e^{\gamma}/3)t^2$. As $t \to 1$, $B_{c2}(T)/B_{c2}(0) \to (8e^{\gamma}/\pi^2)(1-t) = 1.444(1-t)$. Note that this result is consistent with what Helfand and Werthamer[93] found for their normalized field $h^*(0) = B_{c2}(0)/(dB_{c2}/dt)_{t=1} = 0.69 = 1/1.444$ in the dirty limit. Since $\xi(T) \to \sqrt{\pi^3 e^{-\gamma}/24}\sqrt{\xi_0\ell}/\sqrt{1-t} = 0.852\sqrt{\xi_0\ell}/\sqrt{1-t}$, we have in this limit $\lambda_0(T)/\xi(T) = \kappa = \sqrt{42\zeta(3)/\pi^4}\lambda_L(0)/\ell = 0.720\lambda_L(0)/\ell$.

A plot of $B_{c2}(T)/B_{c2}(0)$ is equivalent to a plot of $[\xi(0)/\xi(T)]^2$, as shown in Fig. 12. Moreover, comparing Eqs. (C9) and (C9) with Eqs. (C5) and (34), we see that $q_m(T) = 1/\xi(T)$ and $q_m(0) = 1/\xi(0)$, and for all temperatures we have

$$\frac{B_{c2}(T)}{B_{c2}(0)} = \frac{\xi^2(0)}{\xi^2(T)} = \frac{q_m^2(T)}{q_m^2(0)}. \quad \text{(C11)}$$

APPENDIX D: WORK DONE AND FREE-ENERGY CHANGES RESULTING FROM CURRENT CHANGES

It is of interest to examine the changes in energy as the current increases from zero to some final value. The work done per unit volume is

$$W_v = \int_0^t j_{sq'}E\,dt' = -\left(\frac{\phi_0}{2\pi}\right)\int_0^q j_{sq'}\,dq', \quad \text{(D1)}$$

which is equal to the change in the free-energy density, as we show in the following.

The free-energy density $\Omega_q(T) = F_S(T) - F_N(T)$ of a current-carrying superconductor relative to the energy density of the normal state can be obtained by taking advantage of the theoretical similarities to the problem of superconducting alloys containing paramagnetic impurities. The expression for $\Omega_q(T) = F_S(T) - F_N(T)$ for the latter case obtained by

Skalski *et al.*[32] in their Eq. (5.6) can be rewritten compactly for the current-carrying superconductor as

$$\Omega_q = N(0)\int_0^\infty \mathrm{Re}\left[2p(\omega)+\frac{\Delta_q}{\sqrt{u^2-1}}\right]\tanh\frac{\beta\omega}{2}d\omega, \quad \text{(D2)}$$

using the replacements and changes in notation $\Gamma\to Q$, $\Delta(T,\Gamma)\to\Delta_q(T)$, $N_0\to N(0)$, and $\omega_D'\to\infty$ (weak-coupling limit). Here, $\beta=1/k_BT$,

$$\frac{\omega}{\Delta_q}=u\left(1-i\frac{\zeta}{\sqrt{u^2-1}}\right), \quad \text{(D3)}$$

and

$$p(\omega)=-\int_\omega^\infty\left[\frac{u'}{\sqrt{u'^2-1}}-1\right]d\omega' \quad \text{(D4)}$$

$$=\Delta_q\left[\left(1-i\frac{\zeta}{\sqrt{u^2-1}}\right)(\sqrt{u^2-1}-u)-i\frac{\zeta}{2(u^2-1)}\right] \quad \text{(D5)}$$

is a quantity arising from partial integration of the term proportional to $\ln(1+e^{-\beta\omega})$ in the entropy contribution to $\Omega_q(T)$. Some useful relations are $\mathrm{Re}[p(0)]=0$ and

$$\int_0^\infty \mathrm{Re}\left[p(\omega)+\omega\left(\frac{u}{(u^2-1)^{1/2}}-1\right)\right]=-\frac{\Delta_q^2}{2}. \quad \text{(D6)}$$

The quantity within the brackets in the integrand of Eq. (D2) can be expressed in terms of u as

$$\omega\left(\frac{2\sqrt{u^2-1}}{u}-2+\frac{1}{u\sqrt{u^2-1}}\right), \quad \text{(D7)}$$

and the integral in Eq. (D2) can be evaluated using contour integration around the boundaries of the first quadrant of the complex ω plane, taking into account the poles along the imaginary axis at the Matsubara frequencies $i\omega_n = i2\pi k_BT(n+1/2)=i2\pi k_BT\eta$. The result is

$$\Omega_q(T)=-N(0)(2\pi k_BT)^2\sum_{n=0}^\infty\eta\left[2\left(\frac{u_{nq}}{\sqrt{1+u_{nq}^2}}-1\right)+\frac{1}{u_{nq}\sqrt{1+u_{nq}^2}}\right]. \quad \text{(D8)}$$

Differentiation of Eqs. (11) and (D8) with respect to q yields the general result that

$$\frac{d\Omega_q(T)}{dq}=N(0)(2\pi k_BT)\frac{dQ}{dq}\sum_{n=0}^\infty\frac{1}{1+u_{nq}^2} \quad \text{(D9)}$$

$$=-\left(\frac{\phi_0}{2\pi}\right)j_{sq}(T). \quad \text{(D10)}$$

This result agrees with Eq. (D1).

In the zero-temperature limit, the sum in Eq. (D8) can be converted to an integral over η using Eq. (9), with the result[37]

$$\Omega_q(0)=-\frac{N(0)\Delta_q(0)^2}{2}\left(1-\frac{\pi\zeta_0}{2}+\frac{2\zeta_0^2}{3}\right), \quad \zeta_0\leqslant 1 \quad \text{(D11)}$$

$$=-\frac{N(0)\Delta_q(0)^2}{2}\left(1-\frac{\pi\zeta_0}{2}+\frac{2\zeta_0^2}{3}-\frac{(2\zeta_0^2+1)\sqrt{\zeta_0^2-1}}{3\zeta_0}+\zeta_0\tan^{-1}\sqrt{\zeta_0^2-1}\right), \quad \zeta_0\geqslant 1 \quad \text{(D12)}$$

where $\Delta_q(0)$ is given by Eqs. (23) and (24), and ζ_0 by Eq. (25).

It is possible to write the free-energy density as the sum of two terms $\Omega_q(T)=\mathcal{F}_{cq}(T)+\mathcal{F}_{kq}(T)$, where we identify $\mathcal{F}_{cq}(T)$ as the condensation-energy density and $\mathcal{F}_{kq}(T)$ as the kinetic-energy density:

$$\mathcal{F}_{cq}(T)=-N(0)(2\pi k_BT)\sum_{n=0}^\infty\left[2\hbar\omega_n\left(\frac{u_{nq}}{\sqrt{1+u_{nq}^2}}-1\right)+\frac{\Delta_q}{\sqrt{1+u_{nq}^2}}\right], \quad \text{(D13)}$$

$$\mathcal{F}_{kq}(T)=N(0)(2\pi k_BT)Q\sum_{n=0}^\infty\frac{1}{1+u_{nq}^2}. \quad \text{(D14)}$$

Note, however, that both terms depend upon q and interact. As q increases from zero, $\mathcal{F}_{kq}(T)$ initially increases from zero and the magnitude of $\mathcal{F}_{cq}(T)$ decreases, but their sum $\Omega_q(T)$ decreases to zero as $q\to q_m(T)$. Figure 14 shows the q dependence of the energy densities Ω_q, $\mathcal{F}_{cq}$, and $\mathcal{F}_{kq}$ at $T=0$. It is important to note that $\mathcal{F}_{kq}(T)$ is *not* equal to $\mathcal{L}_k(q,T)j_{sq}^2/2$ except in the limit as $q\to 0$ [see Eq. (1)].

The bulk thermodynamic critical field $H_c(T)$ is defined via the superconducting condensation energy at $q=0$:

$$\tfrac{1}{2}\mu_0H_c^2(T)=-\Omega_0(T) \quad \text{(D15)}$$

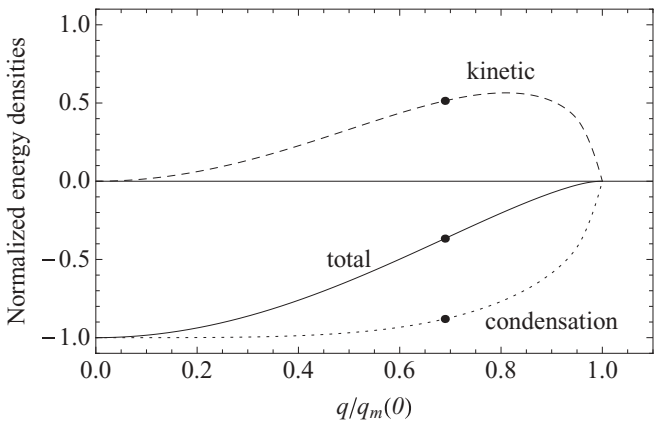

FIG. 14. Energy densities at $T=0$: $\Omega_q(0)$ [solid curve, Eqs. (D11) and (D12)], $\mathcal{F}_{cq}(0)$ [dotted curve, Eq. (D13)], and $\mathcal{F}_{kq}(0)$ [dashed curve, Eq. (D14)], normalized to $N(0)\Delta_0^2(0)/2$. The black points identify the values of these energy densities at $q_d/q_m(0)=0.689$, where $\Omega_q(0)$ has its maximum slope and the depairing-current density is achieved.

$$= N(0)(2\pi k_B T)^2 \sum_{n=0}^{\infty} \left(2\sqrt{\eta^2 + \epsilon_0^2} - 2\eta - \frac{\epsilon_0^2}{\sqrt{\eta^2 + \epsilon_0^2}} \right), \tag{D16}$$

where $\eta = n + 1/2$ and $\epsilon_0 = \Delta_0(T)/2\pi k_B T$. Equation (D16), which follows from Eq. (D8) when $q \to 0$ and $u_{nq} \to u_{n0} = \eta/\epsilon_0$ [see Eq. (9)], reproduces the BCS (Ref. 50) temperature dependence of $H_c(T)$.

[1] G. N. Gol'tsman, O. Okunev, G. Chulkova, A. Lipatov, A. Semenov, K. Smirnov, B. Voronov, A. Dzardanov, C. Williams, and R. Sobolewski, Appl. Phys. Lett. **79**, 705 (2001).

[2] A. J. Annunziata, D. F. Santavicca, L. Frunzio, G. Catelani, M. J. Rooks, A. Frydman, and D. E. Prober, Nanotechnology **21**, 445202 (2010).

[3] For a review, see C. M. Natarajan, M. G. Tanner, and R. H. Hadfield, Supercond. Sci. Technol. **25**, 063001 (2012).

[4] J. R. Clem and E. H. Brandt, Phys. Rev. B **72**, 174511 (2005).

[5] R. Meservey and P. M. Tedrow, J. Appl. Phys. **40**, 2028 (1969).

[6] K. Yoshida, M. S. Hossain, T. Kisu, K. Enpuku, and K. Yamafuji, Jpn. J. Appl. Phys., Part 1 **31**, 3844 (1992).

[7] R. H. Hadfield, A. J. Miller, S. W. Nam, R. L. Kautz, and R. E. Schwall, Appl. Phys. Lett. **87**, 203505 (2005).

[8] A. J. Kerman, E. A. Dauler, W. E. Keicher, J. K. W. Yang, K. K. Berggren, G. Gol'tsman, and B. Voronov, Appl. Phys. Lett. **88**, 111116 (2006).

[9] A. J. Kerman, E. A. Dauler, J. K. W. Yang, K. M. Rosfjord, V. Anant, K. K. Berggren, G. Gol'tsman, and B. M. Voronov, Appl. Phys. Lett. **90**, 101110 (2007).

[10] T. Dahm and D. J. Scalapino, J. Appl. Phys. **81**, 2002 (1997).

[11] P. K. Day, H. G. LeDuc, B. A. Mazin, A. Vayonakis, and J. Zmuidzinas, Nature (London) **425**, 817 (2003).

[12] E. H. Brandt and J. R. Clem, Phys. Rev. B **69**, 184509 (2004).

[13] S. M. Anlage, H. J. Snortland, and M. R. Beasley, IEEE Trans. Magn. **25**, 1388 (1989).

[14] K. Enpuku, H. Moritaka, H. Inokuchi, T. Kisu, and M. Takeo, Jpn. J. Appl. Phys. **34**, L675 (1995).

[15] L. N. Bulaevskii, M. J. Graf, C. D. Batista, and V. G. Kogan, Phys. Rev. B **83**, 144 (2011).

[16] L. N. Bulaevskii, M. J. Graf, and V. G. Kogan, Phys. Rev. B **85**, 014505 (2012).

[17] R. H. Hadfield, Nat. Photonics **3**, 696 (2009).

[18] H. Bartolf, A. Engel, A. Schilling, K. Il'in, M. Siegel, H.-W. Hübers, and A. Semenov, Phys. Rev. B **81**, 024502 (2010).

[19] H. L. Hortensius, E. F. C. Driessen, T. M. Klapwijk, K. K. Berggren, and J. R. Clem, Appl. Phys. Lett. **100**, 182602 (2012).

[20] A. Engel, A. Aeschbacher, K. Inderbitzin, A. Schilling, K. Il'in, M. Hofherr, M. Siegel, A. Semenov, and H.-W. Hübers, Appl. Phys. Lett. **100**, 062601 (2012).

[21] A. Engel, A. Schilling, K. Il'in, and M. Siegel, Phys. Rev. B **86**, 140506(R) (2012).

[22] J. Pearl, Appl. Phys. Lett. **5**, 65 (1964).

[23] J. R. Clem and K. K. Berggren, Phys. Rev. B **84**, 174510 (2011).

[24] M. Tinkham, *Introduction to Superconductivity*, 2nd ed. (McGraw-Hill, New York, 1996).

[25] Here, we discuss the flow of electrons, but instead we could have discussed the flow of Cooper pairs of density $n_s^* = n_s/2$, charge magnitude $e^* = 2e$, and mass $m^* = 2m$. This would have yielded expressions such as $\mu_0 \lambda_0^2(T) = m^*/n_{s0}^*(T)e^{*2}$ and $j_{sq} = -n_{sq}^* e^* v_s$.

[26] J. Y. Lee and T. Lemberger, Appl. Phys. Lett. **62**, 2419 (1993).

[27] K. Maki, Prog. Theor. Phys. **29**, 10 (1963).

[28] K. Maki, Prog. Theor. Phys. **29**, 333 (1963).

[29] K. Maki, Prog. Theor. Phys. **31**, 731 (1964).

[30] A. A. Abrikosov and L. P. Gor'kov, Zh. Eksp. Teor. Fiz. **39**, 1781 (1960) [Sov. Phys.–JETP **12**, 1243 (1961)].

[31] K. Maki and P. Fulde, Phys. Rev. **140**, A 1586 (1965).

[32] S. Skalski, O. Betbeder-Matibet, and P. R. Weiss, Phys. Rev. **136**, A 1500 (1964).

[33] V. Ambegaokar and A. Griffin, Phys. Rev. **137**, A1151 (1965).

[34] S. B. Nam, Phys. Rev. **156**, 470 (1967).

[35] S. B. Nam, Phys. Rev. **156**, 487 (1967).

[36] S. B. Nam, Phys. Rev. B **2**, 3812(E) (1970).

[37] K. Maki, in *Superconductivity*, edited by R. D. Parks, Vol. 2 (Dekker, New York, 1969), p. 1068.

[38] M. Yu. Kupriyanov and V. F. Lukichev, Fiz. Nizk. Temp. **6**, 445 (1980) [Sov. J. Low Temp. Phys. **6**, 210 (1980)].

[39] J. Romijn, T. M. Klapwijk, M. J. Renne, and J. E. Mooij, Phys. Rev. B **26**, 3648 (1982).

[40] A. Anthore, H. Pothier, and D. Esteve, Phys. Rev. Lett. **90**, 127001 (2003).

[41] A. V. Semenov, I. A. Devyatov, and M. Y. Kupriyanov, JETP Lett. **88**, 441 (2008).

[42] N. Groll, A. Gurevich, and I. Chiorescu, Phys. Rev. B **81**, 020504(R) (2010).

[43] G. Eilenberger, Z. Phys. **214**, 195 (1968).

[44] K. Usadel, Phys. Rev. Lett. **25**, 507 (1970).

[45] N. B. Kopnin, *Theory of Nonequilibrium Superconductivity* (Clarendon, Oxford, 2001).

[46] S. B. Kaplan, C. C. Chi, D. N. Langenberg, J. J. Chang, S. Jafarey, and D. J. Scalapino, Phys. Rev. B **14**, 4854 (1976).

[47] P. Fulde and R. A. Ferrell, Phys. Rev. **131**, 2457 (1963).

[48] A. K. Bhatnagar and E. A. Stern, Phys. Rev. Lett. **21**, 1061 (1968).

[49] A. K. Bhatnagar and E. A. Stern, Phys. Rev. B **8**, 1061 (1973).

[50] J. Bardeen, L. N. Cooper, and J. R. Schrieffer, Phys. Rev. **108**, 1175 (1957).

[51] J. Bardeen, Rev. Mod. Phys. **34**, 667 (1962).

[52] M. N. Kunchur, J. Phys.: Condens. Matter **16**, R1183 (2004).

[53] L. P. Gor'kov, Zh. Eksp. Teor. Fiz. **34**, 735 (1958) [Sov. Phys.–JETP **7**, 505 (1958)]; Zh. Eksp. Teor. Fiz. **36**, 1918 (1959) [Sov. Phys.–JETP **9**, 1364 (1959)].

[54] V. L. Ginzburg and L. D. Landau, Zh. Eksp. Teor. Fiz. **20**, 1064 (1950); A complete English translation is available in L. D. Landau, *Men of Physics*, edited by D. ter Haar, Vol. 1 (Pergamon Press, New York, 1965), pp. 138–167.

[55] When $\nabla \cdot \boldsymbol{j}_s = 0$, the conditions $P = 0$ and $E = -dA_s/dt$ hold within the generalized time-dependent GL theory (Ref. 45), and we assume that these conditions also apply here.

[56] This definition of the inductivity is the natural extension of the definition of the inductance L via $V = L\,dI/dt$ relating the voltage drop V across an inductor to the current I.

[57]L. P. Gor'kov and G. M. Eliashberg, Zh. Eksp. Teor. Fiz. **54**, 612 (1968) [Sov. Phys.–JETP **27**, 328 (1968)].
[58]M. Tinkham, Phys. Rev. Lett. **13**, 804 (1964).
[59]A. Schmid, Phys. Kondens. Mater. **5**, 302 (1966).
[60]L. P. Gor'kov and N. B. Kopnin, Sov. Phys.–Usp. **18**, 496 (1975).
[61]A. T. Dorsey, Phys. Rev. B **46**, 8376 (1992).
[62]F. Marsiglio, Phys. Rev. B **44**, 5373 (1991).
[63]D. C. Mattis and J. Bardeen, Phys. Rev. **11**, 412 (1958).
[64]J. R. Clem, Ann. Phys. (NY) **40**, 268 (1966).
[65]K. Holczer, O. Klein, and G. Grüner, Solid State Commun. **78**, 875 (1991).
[66]K. Holczer, L. Forro, L. Mihály, and G. Grüner, Phys. Rev. Lett. **67**, 152 (1991).
[67]O. Klein, E. J. Nicol, K. Holczer, and G. Grüner, Phys. Rev. B **50**, 6307 (1994).
[68]B. B. Jin, T. Dahm, A. I. Gubin, E.-M. Choi, H. J. Kim, Sung-IK Lee, W. N. Kang, and N. Klein, Phys. Rev. Lett. **91**, 127006 (2003).
[69]G. M. Eliashberg, Zh. Eksp. Teor. Fiz. **38**, 996 (1960) [Sov. Phys. JETP **11**, 696 (1960)].
[70]K. Maki, Phys. Rev. **153**, 428 (1967).
[71]S. Sridhar and J. E. Mercereau, Phys. Rev. B **34**, 203 (1986).
[72]We are grateful to S. M. Anlage for this suggestion.
[73]J. R. Clem, Y. Mawatari, G. R. Berdiyorov, and F. M. Peeters, Phys. Rev. B **85**, 144511 (2012).
[74]D. Henrich, P. Reichensperger, M. Hofnerr, K. Il'in, M. Siegel, A. Semenov, A. Zotova, and D. Y. Vodolazov, Phys. Rev. B **86**, 144504 (2012).
[75]M. K. Akhlaghi, H. Atikian, A. Eftekharian, M. Loncar, and A. H. Majedi, arXiv:1205.4290.
[76]G. R. Berdiyorov, M. V. Milosević, and F. M. Peeters, arXiv:1206.4298.
[77]J. S. Langer and V. Ambegaokar, Phys. Rev. **164**, 498 (1967).
[78]D. E. McCumber and B. I. Halperin, Phys. Rev. B **1**, 1054 (1970).
[79]F. Tafuri, J. R. Kirtley, D. Born, D. Stornaiuolo, P. G. Medaglia, G. Balestrino, and V. G. Kogan, Europhys. Lett. **73**, 948 (2006).
[80]M. W. Johnson and A. M. Kadin, IEEE Trans. Appl. Supercond. **7**, 3492 (1997).
[81]M. W. Johnson and A. M. Kadin, Phys. Rev. B **57**, 3593 (1998).
[82]J. R. Clem, in *Low Temperature Physics - LT14*, edited by M. Krusius and M. Vuorio, Vol. 2 (North-Holland, Amsterdam, 1975), p. 285.
[83]J. R. Clem, Phys. Rev. B **12**, 1742 (1975).
[84]J. W. Ekin and J. R. Clem, Phys. Rev. B **12**, 1753 (1975).
[85]Z. Hao, J. R. Clem, M. W. McElfresh, L. Civale, A. P. Malozemoff, and F. Holtzberg, Phys. Rev. B **43**, 2844 (1991).
[86]E. H. Brandt, Phys. Rev. B **34**, 6514 (1986).
[87]A. Yaouanc, P. Dalmas de Réotier, and E. H. Brandt, Phys. Rev. B **55**, 11107 (1997).
[88]J. E. Sonier, Rep. Prog. Phys. **70**, 1717 (2007).
[89]R. V. A. Srivistava and W. Teizer, Solid State Commun. **145**, 512 (2008).
[90]B. Mühlschlegel, Z. Phys. **155**, 313 (1959).
[91]A. A. Abrikosov, L. P. Gor'kov, and I. E. Dzyaloshinskii, *Quantum Field Theoretical Methods in Statistical Physics* (Pergamon, New York, 1965).
[92]D. Saint-James, E. J. Thomas, and G. Sarma, *Type II Superconductivity* (Pergamon, Oxford, 1969).
[93]E. Helfand and N. R. Werthamer, Phys. Rev. **147**, 288 (1966).